



# 1 Quantitative imaging datasets of micro to mesoplankton 2 communities and surface microplastic across the Pacific Ocean 3 from the Tara Pacific Expedition 4

5 Zoé Mériquet<sup>1</sup>, Guillaume Bourdin<sup>2</sup>, Nathaniel Kristan<sup>2</sup>, Laetitia Jalabert<sup>3</sup>, Olivier Bun<sup>1</sup>, Marc Picheral<sup>3</sup>, Louis  
6 Caray-Counil<sup>1</sup>, Juliette Maury<sup>1</sup>, Maria-Luiza Pedrotti<sup>1</sup>, Amanda Elineau<sup>3</sup>, David A. Paz-Garcia<sup>4</sup>, Lee Karp-Boss<sup>2</sup>,  
7 Gaby Gorsky<sup>1</sup>, Fabien Lombard<sup>1</sup> and Tara Pacific Consortium Coordinators team<sup>+</sup>  
8

9 <sup>1</sup>Laboratoire d’Océanographie de Villefranche-sur-Mer, Sorbonne Université, CNRS, France

10 <sup>2</sup>School of Marine Sciences, University of Maine, Orono, Maine 04401, USA

11 <sup>3</sup>Sorbonne Université, CNRS, Institut de la Mer de Villefranche, IMEV, 06230 Villefranche-sur-Mer, France

12 <sup>4</sup>Laboratorio de Genética para la Conservación, Centro de Investigaciones Biológicas del Noroeste, Baja  
13 California Sur 23096, México.

14 <sup>+</sup>A full list of authors appears at the end of the paper.  
15

16 *Correspondence to:* Zoé Mériquet (zoe.meriguet@imev-mer.fr) and Fabien Lombard (fabien.lombard@imev-  
17 mer.fr)

18 **Abstract.** This paper presents the quantitative imaging datasets collected during the Tara Pacific Expedition  
19 (2016-2018) on the schooner Tara. The datasets cover a wide range of plankton sizes, from micro-phytoplankton  
20 > 20 µm to meso-zooplankton of a few cm, as well as non-living particles such as plastic and detrital particles. It  
21 consists of surface samples collected across the North and South Pacific Ocean from open ocean stations (a total  
22 of 357 samples) and from stations located in coastal waters, lagoons or reefs of 32 Pacific islands (a total of 228  
23 samples). As this expedition involved long distances and long sailing times, we designed two sampling systems  
24 to collect plankton while sailing at speeds up to 9 knots. To sample microplankton, surface water was pumped  
25 onboard using a customised pumping system and filtered through a 20 µm mesh size plankton net (here after  
26 Deck-Net (DN). A High Speed Net (HSN; 330 µm mesh size) was developed to sample the mesoplankton. In  
27 addition, a Manta net (330 µm) was also used when possible, to collect mesoplankton and plastics simultaneously.  
28 We could not deploy these nets in reef and lagoon stations of islands. Instead, two Bongo nets (20 µm) attached  
29 to an underwater scooter were used to sample microplankton. Microplankton (20-200 µm) from the DN and Bongo  
30 nets was imaged directly on-board Tara using the FlowCam (Fluid imaging, Inc.) while the mesoplankton (> 200  
31 µm) from the HSN and Manta nets was analyzed in the laboratory with the ZooScan system. Organisms and other  
32 particles were taxonomically and morphologically classified using the web application EcoTaxa automatic sorting  
33 tools, followed by taxonomic expert validation or correction. More than 300 different taxonomic and  
34 morphological groups were identified. The datasets include the metadata with the raw data from which  
35 morphological traits such as size (ESD) and biovolume have been calculated for each particle, as well as a number  
36 of quantitative descriptors of the surface plankton communities. These include abundance, biovolumes, Shannon  
37 diversity index and normalised biovolume size spectra, allowing the study of their structures (e.g. taxonomic,  
38 functional, size structure, trophic structure, etc.) according to a wide range of environmental parameters at the  
39 basin scale. In addition to describing and presenting the datasets, the complementary aim of this paper is to  
40 investigate and quantify the potential sampling biases associated with the two high speed sampling systems and  
41 the different net types, in order to improve further ecological interpretations.

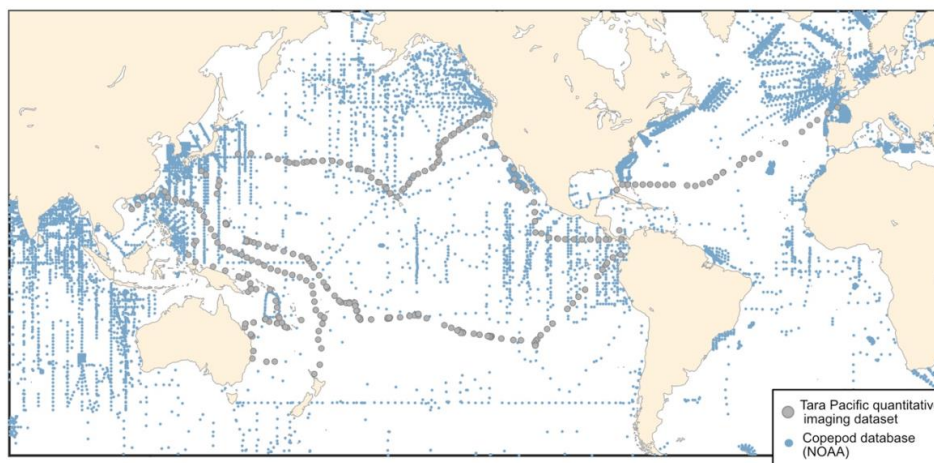
## 42 1. Introduction

43

44 Zooplankton serve as an important conduit for the transfer of energy from primary producers to higher trophic  
45 levels (Ikeda, 1985). In this key position in the trophic chain, they also play an important ecological and



46 biogeochemical role (Turner, 2015; Steinberg and Landry, 2017), with associated socio-economic interests. The  
47 datasets we propose here, covers a wide diversity of surface plankton from 20  $\mu\text{m}$  size at the scale of the Pacific  
48 Ocean. The vastness and unique characteristics of the Pacific Ocean make it a particularly rich study area. From  
49 nutrient-rich upwelling or islands zones to oligotrophic gyres, the diverse oceanic processes of the Pacific Ocean  
50 present a wide range of environmental conditions that significantly influence plankton communities, making it a  
51 key region for plankton research (Chavez et al., 2011; Longhurst, 2007). However, sampling efforts of  
52 zooplankton in the Pacific Ocean largely focused on the temperate North Pacific, eastern and western boundary  
53 currents in the North Pacific, leaving vast areas under-sampled (Drago et al., 2022). This gap is particularly evident  
54 in the NOAA zooplankton dataset (<https://www.st.nmfs.noaa.gov/copepod/atlas>), where the under-sampling is  
55 particularly true for the central subtropical and tropical Pacific where fisheries are important resources for the  
56 thousands of pacific islands. We present a map (Fig. 1) overlaying updated zooplankton databases with samples  
57 from the Tara Pacific expedition, illustrating how these new data address sampling gaps. Global mapping of  
58 zooplankton in the Pacific is hindered by the highly expansive operational ship time face to this vast ocean. The  
59 use of high-speed sampling, such as the Continuous Plankton Recorder (CPR, by Hardy in 1926), the LHPR  
60 (Longhurst et al., 1966), the Gulf III OCEAN Sampler (Gehringer, 1958), the Gulf V plankton sampler (Sameoto  
61 et al., 2000), as well as newer low-tech designs (CSN in Von Ammon et al., 2020; Coryphaena in Mériquet et al.,  
62 2022), including the one employed in our datasets, provides valuable opportunities to expand sampling coverage  
63 and frequency and thus address this undersampling. In the hope of increasing similar cruising speed zooplankton  
64 sampling efforts, we discuss the benefits, challenges and limitations of this high-speed sampling approach based  
65 on the lessons learned from obtaining these datasets.  
66



67  
68  
69  
70  
71

**Figure 1. Spatial distribution of zooplankton observations from the COPEPOD database (<https://www.st.nmfs.noaa.gov/copepod/>; all groups) is represented by blue points. Plankton imaging data ( $> 20 \mu\text{m}$ ) from the Tara Pacific expedition are shown in grey.**

72  
73  
74  
75  
76  
77  
78  
79  
80

The aim of this paper is therefore to present and discuss this open-access quantitative plankton imaging datasets sampled during the Tara Pacific Expedition (2016-2018), conducted in the Pacific Ocean. In general, the effects of different environmental forcings on plankton are often focusing on one size range of plankton, or on a particular taxonomic or functional type to the exclusion of others. It is often difficult to reconcile different methods of analysis (taxonomic, biogeochemical, genomic) to provide a coherent view of the plankton as a whole. In this respect, quantitative imaging is complementary to other methods to study plankton community composition (e.g. HPLC, flow cytometry, genomics) because it simultaneously provides quantitative measures of abundance, morphology and biovolume (as a proxy for biomass) for different taxonomic groups of plankton organisms



81 (Lombard et al., 2019, Mériguet et al., 2022). The datasets represent a diversity of surface plankton analysed with  
82 the use of two quantitative imaging instruments: 1. the FlowCam (Sieracki et al., 1998), which images  
83 microplankton from 20 to 200  $\mu\text{m}$ , and 2. the ZooScan (Gorsky et al., 2010), which images meso-zooplankton  
84 ( $>200 \mu\text{m}$ ). The dataset also includes the plastics imaged by the ZooScan. The datasets represent a total of 2 356  
85 231 images. As with previous Tara expeditions, organizing and cross-linking the various measurements is a  
86 stepping-stone for true open access science resources following FAIR principles (Findable Accessible  
87 Interoperable and Reusable; Wilkinson et al. 2016). In this effort, the strategy adopted by Tara Pacific is to provide  
88 open access data and early and full releases of the datasets once validated or published. All the samples that make  
89 up these datasets should expand the base of standardised data needed to study basin-scale processes in the Pacific  
90 Ocean. One of the more valuable aspects of the plankton sampling strategy of the Tara Pacific expedition, is the  
91 daily sampling, every  $\sim 150$ -200 nautical miles, crossing a large latitudinal range of different oceanic processes  
92 such as equatorial upwelling, coastal upwelling, eastern boundary current, subtropical gyres... The samples were  
93 collected around 32 coral reef islands or in lagoons and at 132 open ocean stations, traversing different oceanic  
94 provinces. We collected over 357 samples in the open ocean and 228 samples close to the reef or in the lagoon.  
95 This offers a potential avenue for exploring the impact of reef islands on plankton abundance and community  
96 structure, potentially shedding light on the still incompletely understood phenomenon of Islands Mass Effect  
97 (IME; Gove et al., 2016, Messié et al. 2022). In relation to the environmental data from the expedition, published  
98 in open access by Lombard et al. 2023, these datasets can be used for global ecological studies of the quantitative  
99 and qualitative aspects of planktonic communities at the basin-scale processes.

100

101 This 2-year expedition involved long distances and long sailing times, for which we designed two new sampling  
102 systems to collect surface plankton while sailing at a maximum speed of 9 knots. The 'Dolphin' sampler was  
103 designed to pump seawater into a 20  $\mu\text{m}$  net on board, the deck net, while the 'High Speed Net' (HSN) was towed  
104 to collect surface plankton larger than 300  $\mu\text{m}$  in size (see Gorsky et al., 2019 for details). In addition to these  
105 high-speed sampling devices, a Manta net (330  $\mu\text{m}$ ) was also used when possible, to collect mesoplankton and  
106 plastics simultaneously. The Manta and HSN nets must be towed relatively long distances to filter enough volume  
107 to provide quantitative estimates of plankton taxa in oligotrophic waters. The reef and lagoon configuration often  
108 did not allow such long towing distances with these devices, so we adapted the sampling strategy to lagoons using  
109 a Bongo frame fitted with two 20  $\mu\text{m}$  Bongo nets towed by an underwater scooter. A complementary objective of  
110 this paper is to investigate and quantify potential sampling biases associated with the high-sampling devices and  
111 between each net type, in order to improve subsequent ecological interpretations and promote similar cruising  
112 speed zooplankton sampling efforts.

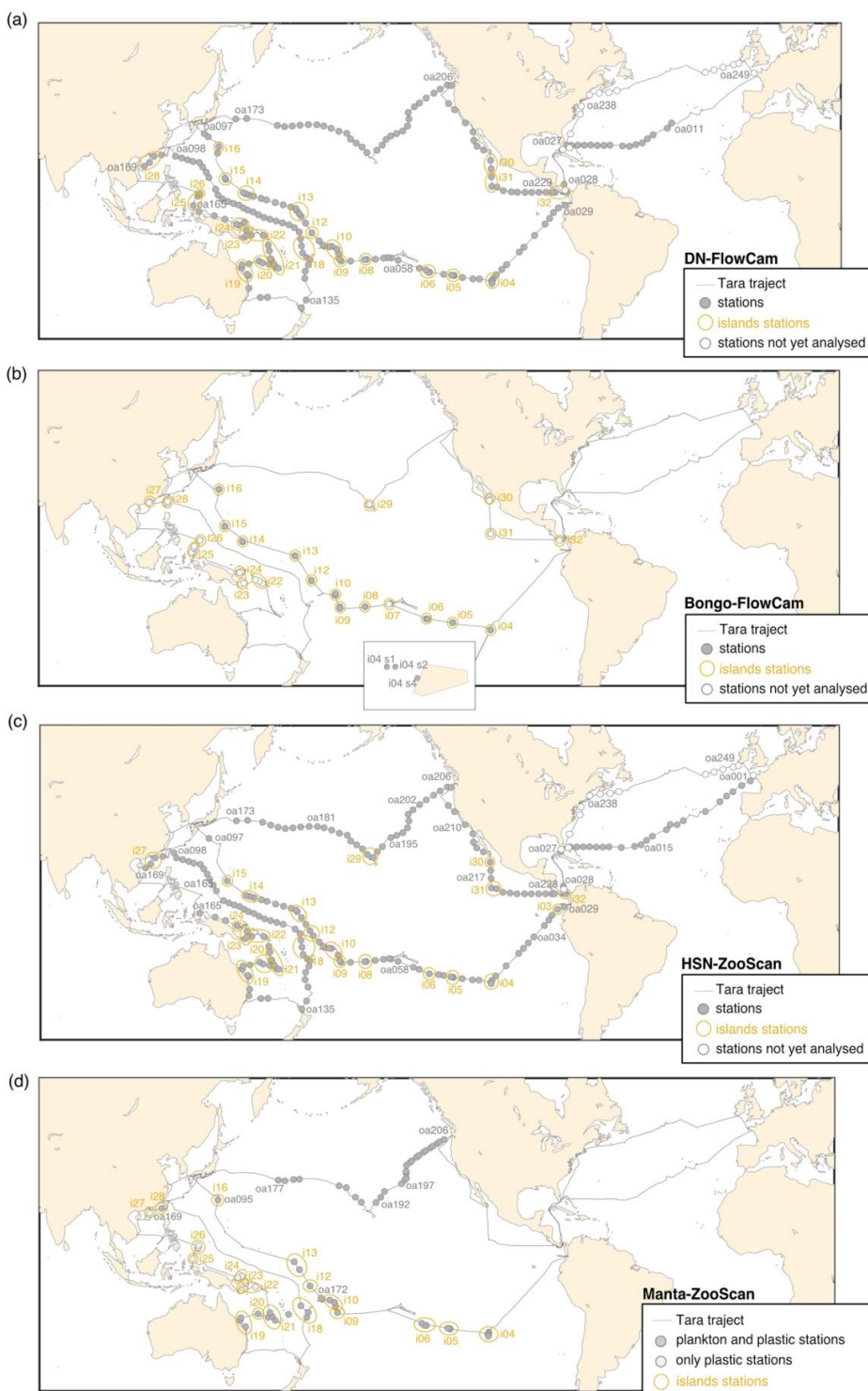
## 113 2. Methods

### 114 2.1 Sampling

115 We present a collection of FlowCam and ZooScan images acquired during the Tara Pacific expedition (2016-  
116 2018; Gorsky et al. 2019, Lombard et al. 2023). All samples and protocol names in this article follow Lombard et  
117 al. (2023) in order to help the user match the samples and associated data presented here with other samples from  
118 the expedition. Sampling was carried out generally at the daily frequency, resulting in a total of 249 sampling  
119 events labelled [oa001] to [oa249] (Fig. 2). The first 28 sampling events occurred during the trans-Atlantic  
120 crossing as the ship sailed from France to the Pacific. At the end of the expedition, the schooner Tara acquired  
121 quantitative imaging samples at stations [oa232] to [oa249] across the North Atlantic. Data are published on the  
122 SEANOE platform to allow for future updates and completion of datasets. The plankton sampling covers a large  
123 latitudinal range (temperate, subtropical, and tropical) as well as a diversity of environments associated with  
124 different oceanic processes (equatorial upwelling, coastal upwelling, eastern boundary current, subtropical gyres,  
125 and other provinces). A selection of 32 coral reef islands systems (labelled [i01] to [i32]) in the tropical and  
126 subtropical Pacific Ocean were targeted for coral reef holobiont studies (Planes et al., 2019), including surface  
127 plankton sampling analysed by quantitative imaging. A summary of geological, topological and human population  
128 characteristics of the different islands targeted (name, size, elevation, human population, etc.) can be found in



129 Lombard et al. (2023). Any sampling event that was conducted within the Exclusive Economic Zone (EEZ) of an  
130 island (defined as the area that stretches 200 nautical miles or 370 km out of the coastline of an island in question)  
131 was considered as an island station and annotated with the island label [i##\_oa###]. All other sampling events  
132 were considered open ocean stations (high seas) and were annotated [i00\_oa###].

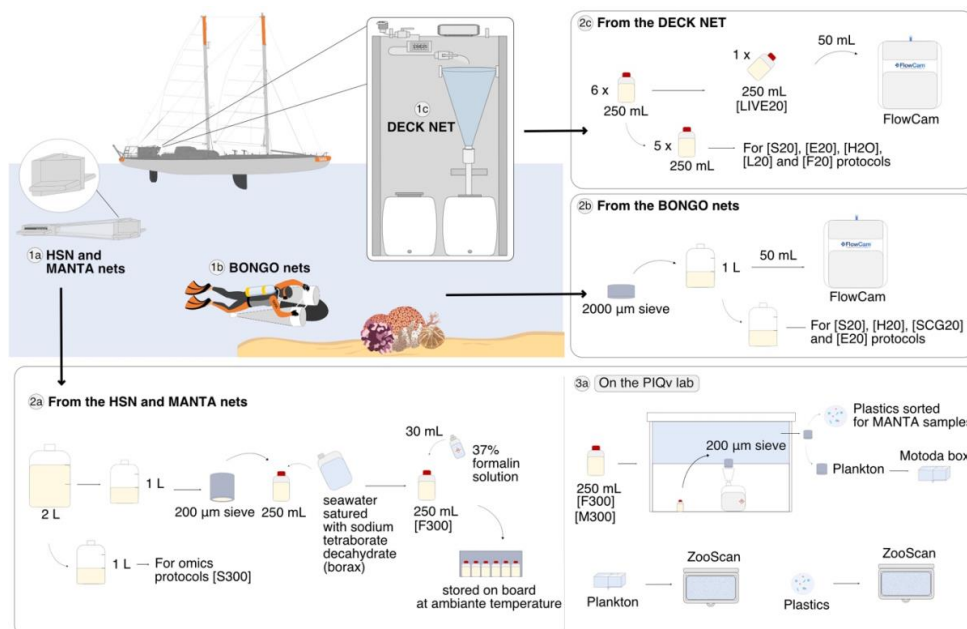




134

135 **Figure 2. Tara Pacific expedition (2016–2018) sampling map for the 4 different datasets: (a) the DN (Deck-Net) -**  
136 **FlowCam, (b) the Bongo Net - FlowCam, (c) the HSN (High-Speed-Net) - ZooScan and (d) the Manta - ZooScan**  
137 **(plankton and plastic samples). Island stations, station within 200 nautical miles of an island, are represented inside a**  
138 **yellow circle. The 'not yet analysed' stations in the figure legend mean that the samples have not yet been scanned for**  
139 **the ZooScan dataset and have not been taxonomically validated for the FlowCam dataset.**

140



141

142

143 **Figure 3. Schematic overview of the sampling events and protocols used during the Tara Pacific expedition for**  
144 **quantitative imaging. The top left panel corresponds to the sampling events with the deployed plankton nets: (1a) the**  
145 **330 µm High Speed Net (HSN) and the 333 µm Manta net, (1b) the 20 µm Bongo nets attached to the underwater**  
146 **scooter and (1c) the 20 µm Deck Net (DN) on the deck of the Tara. Samples from DN (2c) and Bongo (2b) were imaged**  
147 **live with the FlowCam (20–200 µm) and samples from HSN and Manta (2a) were imaged with the ZooScan (> 300 µm).**  
148 **For the ZooScan analysis, samples were fixed using formaldehyde and stored on board and analysed on the Imaging**  
149 **Quantitative Platform (PIQv) in the laboratory in Villefranche-sur-Mer, the protocols in this platform are detailed in**  
150 **the section: "On the PIQv lab" (3a). All sample references are defined in Lombard et al. 2023 (i.e. [S20], [E20], [H20],**  
151 **etc.). Some drawings were taken from Lombard et al. 2023 modified (credit N. Le Bescot).**

### 152 2.1.1 Deck-Net sampling

153 Surface water samples were collected using a custom-built water pumping system named "Dolphin". It consists  
154 of a stainless-steel pyramidal frame with a front aperture of 0.04 m wide and 0.40 m high, deployed from the  
155 starboard of the ship (see pictures in Gorsky et al., 2019). The Dolphin was used underway while sailing and was  
156 connected to a peristaltic pump (max flow rate =  $3 \text{ m}^3 \text{ h}^{-1}$ ) mounted on the deck of the schooner Tara. The system  
157 was equipped with a flowmeter to record flow rates. The pumped water was filtered through a 20 µm net (Deck-  
158 Net) that was mounted on the wall of the wet lab (Fig. 3; 1c and pictures in Gorsky et al., 2019). Before entering the  
159 Deck-Net, the pumped water passes through a 2000 µm mesh filter. Deck-Net pumping lasted 1 to 2 hours,  
160 depending on plankton concentration. Samples were divided into subsamples, which included one subsample for  
161 quantitative micro-plankton imaging analysis on live samples (LIVE20; Fig. 3; 2c) and the remaining for specific



162 protocols detailed in Lombard et al. (2023). Further information on the Dolphin system, the Deck-Net, and various  
163 protocols based on this sampling can be found in Gorsky et al. (2019) and Lombard et al. (2023).

### 164 2.1.2 Bongo nets sampling

165 Plankton larger than 20  $\mu\text{m}$  were sampled at  $\sim 2$  m below the sea surface using two small diameter Bongo plankton  
166 nets with 20  $\mu\text{m}$  mesh size and an opening area of 0.071  $\text{m}^2$ , attached to an underwater scooter (Fig. 3; 1b) and  
167 towed for about 15 min at maximum speed ( $0.69 \pm 0.04 \text{ m s}^{-1}$ ). Each net was equipped with a flowmeter rated to  
168 provide accurate measurements at speeds above  $0.3 \text{ m.s}^{-1}$ , but, the relatively low maximum speed of the  
169 underwater scooter was insufficient to allow seawater to flow through the 20  $\mu\text{m}$  mesh fast enough to trigger the  
170 rotation of the flowmeter. Therefore, volume was estimated from the tow speed and tow duration using the  
171 following Eq. (1):

$$172 \text{ Bongo volume} = 0.071 \times \text{tow speed} \times \text{tow duration} \quad (1)$$

### 173 2.1.3 HSN and Manta nets sampling

174 Simultaneously with the deployment of the Dolphin to collect microplankton, the High Speed Net (HSN) was  
175 towed to sample the mesoplankton. The HSN was equipped with a 330  $\mu\text{m}$  mesh and designed to be deployed  
176 while sailing up to 9 knots (average speed deployment: 6.7 knots). The HSN features the same mouth opening as  
177 the Dolphin system, consisting of a stainless-steel pyramidal frame with a front aperture measuring  $0.40 \times 0.04 \text{ m}$   
178 (see zoom on the HSN mouth system on Fig. 3). The base opening of this pyramidal structure measures  $0.34 \times$   
179  $0.34 \text{ m}$ . This net was deployed from the starboard and towed at a distance of 50–60 m behind the ship (to avoid it  
180 being in the wake of the ship), for a period of 60–90 min (depending on plankton density). In addition to the HSN,  
181 Manta net was also deployed in some locations (Fig. 2). The Manta net have rectangular frame of  $0.16 \times 0.60 \text{ m}$   
182 mouth opening with a 4 m long net with 333  $\mu\text{m}$  mesh size, and was used at a maximum speed of 3 knots, for an  
183 average of 30–40 minutes.

184  
185 Flowmeters were mounted at half of the opening height above the bottom of the opening on both HSN and Manta  
186 nets to ensure it was well submerged during deployment while measuring the filtered volume. Theoretical volumes  
187 were calculated taking into account a 3/4 mouth opening of the HSN and Manta nets,  $0.3 \times 0.04$  and  $0.6 \times 0.12$   
188 m, respectively (see Eq. (3), (4) and (5)). As these nets are surface nets, the water collected actually passed through  
189  $\sim 3/4$  of the opening height (see photos of deployments in Gorsky et al., 2019). To calculate volumes from the  
190 flowmeter for the HSN, we considered an opening of  $0.34 \times 0.34 \text{ m}$ , corresponding to the dimensions of the  
191 pyramid base opening where the flowmeter was positioned inside the HSN (see Eq. (2)). We compared the volume  
192 estimated from the flowmeter readings with theoretical estimation using the towing distances. We computed the  
193 towing distances using the minute binned latitude and longitude recorded with the Tara's GPS along each  
194 deployment. We calculated the distance between the start-end latitude and start-end longitude for each minute, to  
195 calculate the distance per minute covered by the boat. We then summed these 'per-minute' distances over the  
196 duration of the deployment to obtain a calculated distance that is as close as possible to the true towing distance  
197 and accounts for potential modification of the boat's heading during deployments. The equations for calculating  
198 the filtered volumes are therefore as follows:

$$199 \text{ HSN flowmeter volume} = \text{flowmeter end} - \text{flowmeter start} \times 0.3 \times (0.34 \times 0.34) \quad (2)$$

$$200 \text{ HSN theoretical volume} = \text{tow distance} \times (0.3 \times 0.04) \quad (3)$$

$$201 \text{ Manta flowmeter volume} = \text{flowmeter end} - \text{flowmeter start} \times 0.3 \times (0.6 \times 0.12) \quad (4)$$

$$202 \text{ Manta theoretical volume} = \text{tow distance} \times (0.6 \times 0.12) \quad (5)$$

203 Simplified Metadata in csv provides both flowmeters and theoretical volumes for HSN and Manta net, enabling  
204 the user to select the filtered volume for the calculation of quantitative descriptors. A discussion of the biases  
205 associated with each estimate is given in section 3.2. The filtered volumes uploaded as metadata in EcoTaxa



206 (EcoTaxa export table in tsv, see part 2.5) and used to compute quantitative descriptors (see part 2.5) are the  
207 theoretical volumes calculated from the distance (see the results of technical validation part 3.2.1).

208

209 Once recovered, samples collected both by the HSN net and the Manta net followed the same procedure (Fig. 3;  
210 2a). The sample was divided into two 1 L fractions (details in Gorsky et al., 2019). One fraction was concentrated  
211 on a 200 µm sieve and resuspended in a 250 mL double-sealed bottle using filtered seawater saturated with sodium  
212 tetraborate decahydrate (borax), fixed with 30 mL of 37% formalin solution and stored at room temperature for  
213 taxonomic and morphological analysis by imaging methods in the laboratory (samples named [F300]). The other  
214 fraction was used for omic analysis.

## 215 **2.2 Acquisition and treatment of plankton imaging data**

216 Sample labels were annotated by different users at different times during the expedition and are therefore not  
217 homogeneous. In order to avoid confusion or misunderstanding of the labelling of the samples, an additional  
218 column has been created in the csv Simplified Metadata (column “Homogenous sample names”) with  
219 homogeneous names for all datasets.

### 220 **2.2.1 FlowCam analysis**

221 Samples from the Deck-Net (250 mL) and Bongo net (50mL) were imaged live directly on board using a FlowCam  
222 Benchtop B2 series (Fluid Imaging Technologies; Sieracki et al., 1998) equipped with a ×4 objective and a 300  
223 µm deep glass flow cell to examine the micro-plankton samples (size range 20-200 µm; Fig. 3; 2c). Each sample  
224 was first passed through a 200 µm sieve to remove large objects that could clog the FlowCam imaging cell.  
225 Samples were then diluted or concentrated to achieve optimum object flow. The auto-image mode was used to  
226 image the particles in the focal plane at a constant flow rate.

### 227 **2.2.2 ZooScan analysis**

228 The ZooScan imaging instrument (Gorsky et al. 2010) was used to study the mesoplankton. Samples collected  
229 from the HSN and Manta nets ([F300]) were imaged at the Quantitative Imaging Platform (PIQv) of the Institut  
230 de la Mer de Villefranche (Fig. 3; 3a). In addition, preserved zooplankton samples are stored in the Collection  
231 Center for Plankton of Villefranche (CCPv). The formaldehyde solution was replaced by filtered seawater during  
232 the analysis.

233

#### 234 *Plankton samples analysis from HSN and Manta nets on the ZooScan*

235

236 Before scanning on the ZooScan, plankton samples were divided using a Motoda splitter (Motoda, 1959) to obtain  
237 a concentration of approximately between 1000 and 2500 objects per subsample and scanned with the ZooScan.  
238 This sampling strategy correctly accounted for the many small organisms as well as the large ones that might be  
239 under-sampled when subsampling with the Motoda box. This limit ([1000- 2500] objects) was defined by the  
240 PIQv platform to avoid the overlap of planktonic organisms, while retaining enough organisms to give a reliable  
241 quantitative measurement of the sample. After each scan, a quality control was systematically carried out  
242 concerning i) the quality of the scanned image and ii) the number of objects imaged, to ensure that that the number  
243 of objects is within the limits given above. The quality control tool for imaging data is accessible on the PIQv  
244 website: <https://sites.google.com/view/piqv/>. After treatment in the ZooScan, all samples were re-concentrated on  
245 a 200 µm sieve and resuspended in a 250 mL double-sealed bottle using filtered seawater saturated with borax,  
246 fixed with 30 mL of 37% formalin solution and returned to the CCPv.

247

248 The borax (sodium tetraborate decahydrate) used as a buffer has a tendency to crystallise, forming white crystals.  
249 If the borax solution was not filtered sufficiently, crystals would end up in the plankton samples, digitised and  
250 counted as objects. Thus, if Borax was not filtered sufficiently white crystals could represent a large proportion  
251 of the objects within the 1000-2500 limit and thus bias the quantitative measurement of the plankton. We identified





252 24 samples containing borax crystals during the analysis. Therefore, prior to scanning, these samples were  
253 thoroughly rinsed with filtered seawater through a 300 µm mesh sieve to remove a maximum of borax crystals  
254 from the sample. A 200 µm mesh sieve was placed below the 300 µm sieve in order to conserve the initial sample  
255 in the collection (CCPv). Analysis on the ZooScan was performed from the 300 µm sieve.

256

257 *Plastic sampling from Manta net*

258

259 Samples from the Manta nets were gently transferred to a Petri dish. Plastic-like particles were manually separated  
260 from other components such as wood, zooplankton, and organic tissues (Fig. 3; 3a). Entangled pieces of plastic  
261 were picked up manually from zooplankton and aggregated under a stereoscopic dissecting microscope, using  
262 forceps. The visual criteria used to classify a microfiber as synthetic were the absence of cellular structures and  
263 scales on the surface, a curved shape with a uniform surface, a uniform thickness along the entire length of the  
264 filament, spots, and strong strands (Barrows et al., 2018; Hidalgo-Ruz et al., 2018). Each sample was examined  
265 twice to ensure the detection of most of the plastic particles. Isolated plastic particles were then imaged with  
266 Zooscan. To minimise the plastic contamination of the samples, a quality control approach was undertaken  
267 following the protocol described by Pedrotti et al. (2022).

### 268 **2.3 Images processing**

269 For FlowCam and ZooScan, the full methodology used can be found in their respective manuals  
270 (<https://sites.google.com/view/piqv/piqvmanuals/instruments-manuals>; for the ZooScan the protocol is also  
271 available on zenodo by Jalabert, 2022). Images generated by FlowCam and ZooScan were processed using the  
272 ZooProcess software in ImageJ (Gorsky et al. 2010) which extracts segmented objects as vignettes. During this  
273 process, each vignette was associated with a set of 46 morphometric measurements for object characterization,  
274 including grey levels, fractal dimension, shape and size, which were imported into the EcoTaxa web application  
275 (Picheral et al. 2017) for taxonomic classification. For ZooScan, ZooProcess includes a tool that allows for the  
276 digital separation of possible touching objects in the original image. As touching objects can affect estimates of  
277 abundance and size (Vandromme et al. 2012). Remaining touching objects after the application of the tool were  
278 identified for in all vignettes and objects were separated using the ZooProcess separation tool to improve the  
279 quality of further taxonomic annotation, counts and size structure analysis of zooplankton. A quality control step  
280 on the number of remaining multiples was systematically performed after the taxonomic annotation.

### 281 **2.4 Taxonomic identification**

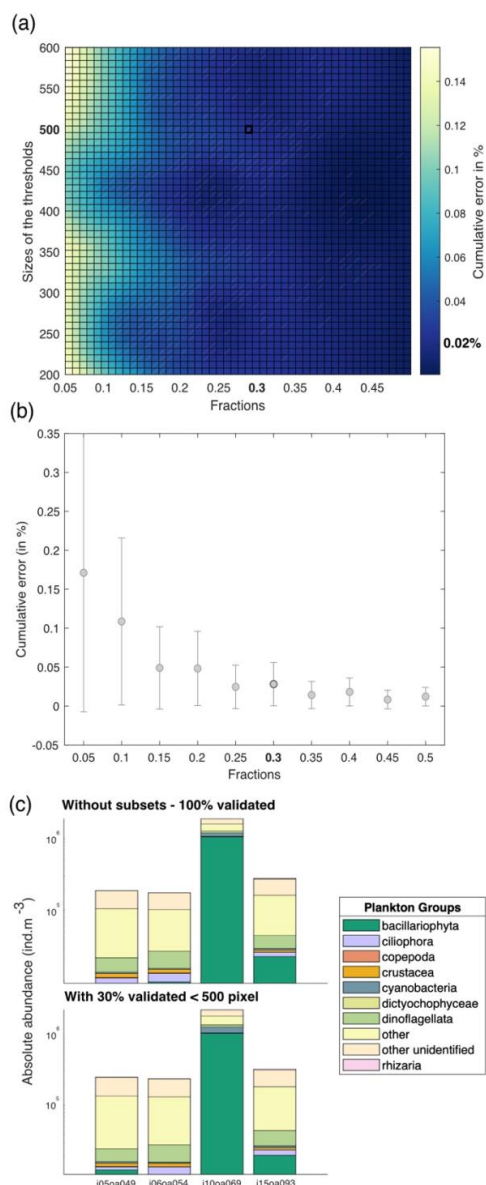
282 Using image recognition algorithms on EcoTaxa, predicted taxonomic categories were validated or corrected by  
283 trained taxonomists. For the majority, the taxonomic classification effort was possible up to the genus and only in  
284 rare cases up to the species. A number of organisms could not be reliably taxonomically identified due to a lack  
285 of identification criteria and were therefore grouped into temporary categories (t00x) following similar  
286 morphological criteria. Nine different trained taxonomists from the PIQv platform annotated FlowCam and  
287 ZooScan vignettes on these datasets. To reduce operator bias between taxonomists and to ensure taxonomic  
288 consistency, a final stage of homogenisation was carried out by two taxonomists after all vignettes had been  
289 validated. At the time of publication of these datasets, copepod genera had not been homogenised for ZooScan,  
290 but homogenisation will be pursued in the future and the published SEANO dataset updated. Annotations of  
291 FlowCam and ZooScan vignettes from the different nets were also done by different taxonomists but the list and  
292 the global criteria to identify a group were common. Overall, these datasets are published on the SEANO flexible  
293 platform that allows updates and corrections, so that taxonomic annotations can be improved over time. All  
294 vignettes with taxonomic annotations are visible on the open access project in EcoTaxa (section 4).

295

296 The Tara Pacific settings for the FlowCam live analysis generates many more images than the ZooScan. For  
297 example, for station oa140, the ZooScan counts 1 435 images compared to 42 915 images for the FlowCam. Given  
298 that taxonomists annotated images on an image-by-image basis, the validation or correction of the automatic  
299 classification on these numerous FlowCam images would require a much higher investment of time than for the



300 ZooScan samples. In addition, the resolution of the FlowCam images of the smallest organisms does not allow us  
301 to classify them properly and at a sufficient precision. Therefore, we validated only 30% of the total images  
302 smaller than 500 pixels (equivalent to  $\sim 45 \mu\text{m}$  in ESD), randomly picked, assuming that this 30% random  
303 subsample leaves a statistical count that is sufficiently representative of the population. Prior to this choice, a  
304 series of tests were conducted to assess the impact of different fraction of image validation at varying object size  
305 thresholds. Samples were randomly selected and 100% of the images were taxonomically validated. Subsequently,  
306 a series of simulations (three times for the four samples, random sampling each time) were conducted to assess  
307 the impact of varying size thresholds (i.e. from 200 to 600 pixels, equivalent to 18 to 55  $\mu\text{m}$ , with a step of 50  
308 pixels) on the proportion of total images to be annotated (fractions from 5% to 50%, with increments of 5%). We  
309 compared the results of these simulations by using the relative Root Mean Square Error (RMSE). The RMSE  
310 values were divided by the total number of 100% validated values and multiplied by 100 to express the cumulative  
311 error as a percentage. Results are shown in Fig. 4 and illustrate the cumulative error across the absolute abundance  
312 values. For our chosen threshold of 500 pixels and subsets at 30% (highlighted in bold on the Fig. 4), we observed  
313 induced errors of 0.02%. In Figure 3d, we present the absolute abundance and taxonomic group composition of  
314 plankton from the four samples that were 100% taxonomically annotated, alongside the same four samples that  
315 were only 30% ( $< 500$  pixels) annotated. These samples show highly comparable results in both absolute  
316 abundance and taxonomic composition (data not shown). We carried out the same analysis as described in Figure  
317 4 for the total size spectrum (NBSS) and the taxonomic composition (relative abundance). They showed an  
318 induced error of 20% and 12%, respectively. The software ZooProcess 8.27, available on the PIQv website, now  
319 includes the capability for subsampling on Flowcam data.



320

321

322 **Figure 4.** (a) Estimated cumulative error associated with partial validation of particles below a size cut-off threshold  
 323 ranging from 200 to 600 pixels and validated fractions ranging from 5% to 50%. Errors are computed as the percentage  
 324 Root Mean Squared Error (RMSE) between fully validated samples and partially validated samples in three different  
 325 metrics for cumulative error in absolute abundance. RMSE values represent the outcomes of simulations, each  
 326 conducted three times for the four samples, with random sampling. (b) Cumulative error according to the Fractions  
 327 chosen. The threshold is fixed at 500 pixels. (c) Comparison between the absolute abundance (ind.m<sup>-3</sup>) and plankton  
 328 group composition for samples taxonomically annotated at 100% and for the same samples annotated at 30% below  
 329 the threshold of 500 pixels, equivalent to 45  $\mu$ m.



330 **2.5 Datasets**

331 **2.5.1 Plankton images on EcoTaxa and the associated tsv.**

332 This paper presents the quantitative imaging datasets collected during the Tara Pacific Expedition. The datasets  
 333 include 4 datasets of microplankton imaged by the FlowCam and sampled by the Deck-Net and the Bongo Nets,  
 334 and mesoplankton imaged by the ZooScan sampled by the HSN and the Manta. All of the sorted images of  
 335 plankton, plastic and particles are visible on the open-access projects on the EcoTaxa web application. The \*.tsv  
 336 files exported from the EcoTaxa platform are provided. Readme tables for FlowCam and ZooScan \*.tsv are also  
 337 provided to facilitate their use.

338 **2.5.2 Quantitative descriptors to study the micro- and meso-plankton community**

339 For each dataset, we designed a table combining the metadata and data from which we have calculated quantitative  
 340 descriptors of planktonic communities: abundance (ind/m<sup>3</sup>), biovolume (mm<sup>3</sup>/m<sup>3</sup>; proxy of biomass) and Shannon  
 341 diversity Index. Abundance (ind/m<sup>3</sup>) and biovolume (mm<sup>3</sup>/m<sup>3</sup>) were calculated taking into account the volume of  
 342 water filtered by the plankton samplers (see formula in Table 1). Biovolumes (in mm<sup>3</sup>/m<sup>3</sup>) were computed using  
 343 area, riddled area, and ellipsoidal measurement of each object, and are available in the \*.csv table (following  
 344 Vandromme et al., 2012; formula in Table 1). For analysis shown here, major and minor axes of the best ellipsoidal  
 345 approximation were used to estimate the biovolume of each object, following the recommendations of  
 346 Vandromme et al. (2012). Size was expressed as equivalent spherical diameter (ESD, μm). Diversity was  
 347 calculated using the Shannon index (H: see formula Table 2). The individual biovolumes of the organisms were  
 348 arranged in Normalised Biomass Size Spectra (NBSS), as described by Platt & Denman (1978), along a harmonic  
 349 range of biovolumes such that the minimum and maximum biovolumes of each class are linked by: B<sub>vmax</sub>= 20.25  
 350 B<sub>vmin</sub>. The NBSS was obtained by dividing the total biovolume of each size class by its biovolume interval  
 351 (B<sub>vrange</sub>=B<sub>vmax</sub>-B<sub>vmin</sub>). The NBSS was representative of the number of organisms (abundance within a factor) per  
 352 size class. This can provide insight into ecosystem structure and function through the 'size spectrum' approach,  
 353 which generalises Elton's pyramid of numbers. The NBSS size spectra of each sample (in abundance/μm) is  
 354 provided in a separated zip files. Tables (.csv). Plankton abundance and biovolume were calculated for each  
 355 taxonomic annotation and for different levels of grouping: living or nonliving, plankton groups and trophic  
 356 association. The full list of these groups linked to all EcoTaxa taxonomic annotations is given in the Table A1 to  
 357 A4 (appendix A) of the taxonomic list and groups in each dataset.  
 358

Descriptors		Formulas for FlowCam	Formulas for ZooScan
<b>Abundance</b> (ind/m <sup>3</sup> ): Number of individus in the sampling/ m <sup>3</sup>		$\frac{(\text{object\_annotation\_category} \times \text{sample\_conc\_vol\_ml})}{(\text{acq\_fluid\_volume\_imaged} \times \text{sample\_initial\_col\_vol\_m3})}$	$\frac{(\text{object\_annotation\_category} \times \text{acq\_sub\_part})}{\text{sample\_tot\_vol}}$
<b>Biovolume</b> (m m <sup>3</sup> / m <sup>3</sup> ): Volume biomass of individus in the sampling/ m <sup>3</sup>	Plain biovolume	$\frac{(4/3 \times \prod \times (\sqrt{(\text{object\_area}) / \prod})^3 \times \text{sample\_conc\_vol\_ml})}{(\text{acq\_fluid\_volume\_imaged} \times \text{sample\_initial\_col\_vol\_m3})}$	$((4/3 \times \prod \times (\sqrt{(\text{object\_area}) / \prod})^3 \times \text{acq\_sub\_part}) / \text{sample\_tot\_vol})$
	Riddled biovolume	$\frac{(4/3 \times \prod \times (\sqrt{(\text{object\_area\_exc} (\text{mm}^2) / \prod)^3 \times \text{sample\_conc\_vol\_ml})}{(\text{acq\_fluid\_volume\_imaged} \times \text{sample\_initial\_col\_vol\_m3})}$	$((4/3 \times \prod \times (\sqrt{(\sqrt{(\text{object\_area\_exc} / \prod)})^3} \times \text{acq\_sub\_part}) / \text{sample\_tot\_vol})$



	Ellipsoid biovolume	$\left(\frac{4}{3} \times \pi \times \left[\left(\frac{\text{object\_major}}{2}\right) \times \left(\frac{\text{object\_minor}}{2}\right) \times \left(\frac{\text{object\_minor}}{2}\right)\right] \times \text{sample\_conc\_vol\_ml} / (\text{acq\_fluid\_volume\_imaged} \times \text{sample\_comment\_or\_volume})\right)$	$\left(\left(\frac{4}{3} \times \pi \times \left[\left(\frac{\text{object\_major}}{2}\right) \times \left(\frac{\text{object\_minor}}{2}\right) \times \left(\frac{\text{object\_minor}}{2}\right)\right]\right) \times \text{acq\_sub\_part} / \text{sample\_tot\_vol}\right)$
<b>Diversity</b> Shannon Indice (H)	$-\sum (\text{abundance relative (\%)} / 100) * \log(\text{abundance relative (\%)} / 100)$		
<p><b>Data description</b></p> <p>object_area : surface area of the object [pixel<sup>2</sup>]              object_area_exc : surface area of the object excluding holes (object_area*(1-(object_%area/100))) [pixel<sup>2</sup>]              object_minor : length of secondary axis of the best fitting ellipse for the object [pixel]              object_major : length of the primary axis of the best fitting ellipse for the object [pixel]</p> <p><b>Data description for FlowCam</b>              See Export EcoTaxa FlowCam read me.csv</p> <p>object_annotation_category : taxon display_name in Ecotaxa              sample_conc_vol_ml : concentrated or diluted water volume (from sample_comment_or_volume) [mL]              acq_fluid_volume_imaged : flowcam total images volume [mL]              sample_initial_col_vol_m3 : initial collected volume, (if nets : sum of the nets) [mL]</p> <p><b>Data description for ZooScan</b>              See Export EcoTaxa ZooScan read me.csv</p> <p>object_annotation_category : taxon display_name in Ecotaxa              acq_sub_part : subsampling division factor of the sieved fraction of the sample              sample_tot_vol : total filtered volume by the sampling gear [m3]</p>			

359  
 360 **Table 1. Formulas used to calculate quantitative variables in datasets. The variable names correspond to the real names**  
 361 **of the variables in the exports (tsv files) and are described in the table.**

362 **3. Technical validation and discussion**

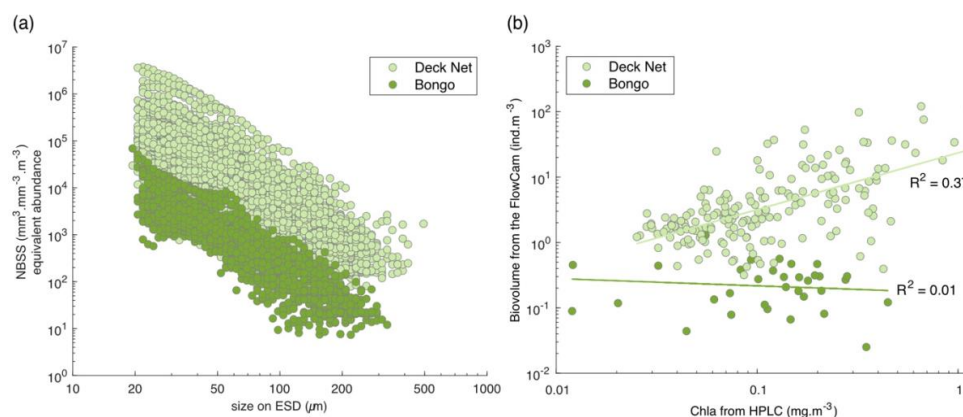
363 **3.1 Limitations of Bongo net sampling for quantitative estimations**

364 Both the Bongo nets and the Deck Net consisted of a 20 µm mesh to collect micro-plankton throughout the  
 365 expedition. The Bongo was deployed on the reef or in the lagoon while the Deck Net was deployed in the open  
 366 ocean. We measured chlorophyll concentration and beam attenuation along the transects passing through the nets  
 367 stations and saw a clear increase when sailing towards an island and in the lagoon (Bourdin et al. in rev). Although  
 368 we expect more plankton concentration on the reef and in the lagoon, many Bongo net samples showed lower  
 369 concentrations than nearby open ocean samples from the Deck Net, as evidenced by the NBSS spectra (Fig. 5a).  
 370 The chlorophyll a (chl<sub>a</sub>) values obtained from the HPLC measurements do not represent the same size classes of  
 371 phytoplankton as those observed with the FlowCam, but we were interested in whether or not there were likely to  
 372 be similar trends in phytoplankton biomass changes measured for the same station (Fig. 5b). Similar trends appear  
 373 to be found for the Deck Net samples, while there is a lack of similar trends for the Bongo. This underestimation



374 of concentration may suggest an overestimation of the volume of Bongo filtered. The divers were fully submerged  
375 in the water, so we assume that the current speed should have had little or no effect on the theoretical volume  
376 estimation. Uncertainty may be associated with the recording of tow duration (maximum 15 minutes), too long  
377 for these net characteristics and such suspended matter concentrations, which would lead to clogging of the nets.  
378 The Bongo nets have a mesh size of 20  $\mu\text{m}$ , an opening area of 0.071  $\text{m}^2$  and an average filtered volume of  $\sim 100$   
379  $\text{m}^3$ . Indeed, calculations from Smith et al. (1968a) give an average ratio of filtration efficiency (filtered area  
380 divided by the mouth area) of  $\sim 1380$ , a value identified by these authors as susceptible to clogging. Therefore, it  
381 is strongly recommended that quantitative imaging Bongo net samples are only used for qualitative purposes or  
382 semi-quantitative analysis.  
383

383



384

385

386 **Figure 5. (a) Comparison of Normalised Biovolume Size Spectra (NBSS; in log-log) of the live plankton between the**  
387 **Bongo nets and the Deck Net. (b) Phytoplankton biovolume ( $\text{ind} \cdot \text{m}^{-3}$ ) estimated from the FlowCam samples, which**  
388 **were collected using the Bongo nets and the Deck Net, according to the Chla values obtained from the HPLC**  
389 **measurements at the same station. The selection of phytoplankton organisms was made possible by taxonomic**  
390 **validation of FlowCam images from these two nets.**

### 391 3.2 Benefits and limitations of high-speed deployment

392 During the Tara Pacific open ocean transects, we decided to take on the challenge of collecting plankton samples  
393 while sailing at speeds of up to 9 knots. This high-speed sampling provides valuable opportunities to expand the  
394 coverage of our sampling with a daily frequency. As a result, one of the most valuable aspects of the Tara Pacific  
395 strategy is the daily collection of samples approximately every 150 to 200 nautical miles, covering a wide range  
396 of oceanic structures across the Pacific basin. This approach is particularly valuable as we aimed for 'end-to-end'  
397 sampling of surface waters (Gorsky et al., 2019) with the micro to macroplankton fractions presented in this  
398 article. However, the constraint of surface sampling and of deploying and retrieving the instruments at cruising  
399 speed forced us to develop new robust, relatively small and user-friendly devices adapted for the Tara schooner.  
400 The combined deployment of the Dolphin system and the High-Speed Net (HSN) designed to this purpose and  
401 present in this article, represents, to our knowledge, the first system enabling discrete sampling of the entire  
402 surface planktonic ecosystem with deployment and retrieval at cruising speeds  $< 9$  knots.  
403

404 The development of the high-speed plankton samplers began in the early 20th century with the well-known  
405 Continuous Plankton Recorder (CPR), developed by Alister Hardy in 1926, which is designed to be towed under  
406 the surface over long distances at speeds up to 25 knots. Following the CPR, other high-speed net systems  
407 emerged, including the Longhurst-Hardy Plankton Recorder (LHPR: Longhurst et al., 1966), Gulf III OCEAN  
408 Sampler (Gehring, 1958), and Gulf V plankton sampler (Sameoto et al., 2000) as well as newer low-tech designs  
409 (CSN in Von Ammon et al., 2020; Coryphaena in Mériquet et al., 2022). All high-speed zooplankton samplers  
410 face the challenge of maintaining filtration efficiency at higher towing speeds. Thus, higher speeds require a larger



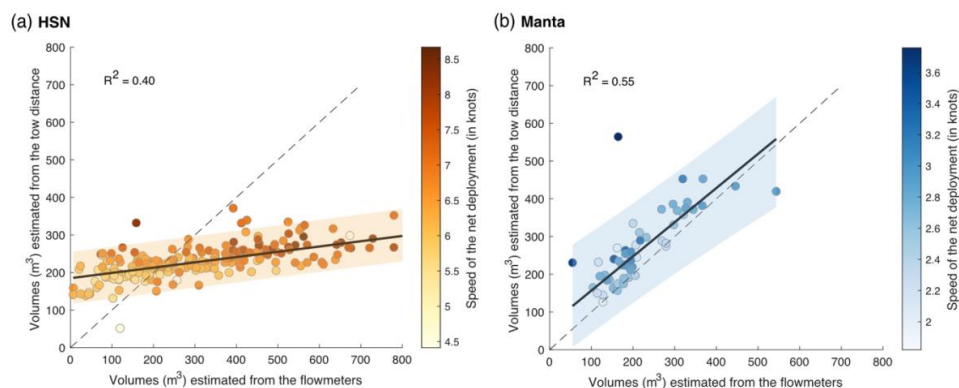
411 relative filtration area to optimises filtration efficiency while minimising excessive pressure on the net and  
412 mitigating the pressure wave that pushes organisms away from the net (Harris et al., 2000; Keen, 2013; Skjoldal  
413 et al., 2013). A critical design principle is therefore to obtain a sufficiently high ratio of mesh filtering area to net  
414 opening area (Smith et al., 1968b; Skjoldal et al., 2013). To achieve this, high-speed zooplankton samplers often  
415 employ a small initial opening area that widens internally (e.g. CPR has an 1.27 cm<sup>2</sup> entrance aperture expanding  
416 to 5cm x 10cm; the use of conic noses on the Gulf-V and LHPR). This design trade-off essential for pressure  
417 reduction, comes at a cost. The small surface area of the mouth opening means a smaller volume filtered, reducing  
418 the probability of collecting less abundant, larger organisms (Skjoldal et al., 2013). The avoidance of active  
419 swimming zooplankton, net opening area size dependent, is also described as the bias affecting the catch of  
420 mesoplankton by Harris et al., 2000. This may be discussed, as increasing tow speed may improve the capture  
421 efficiency of zooplankton capable of active avoidance (Skjoldal et al. 2013). Therefore, high-speed sampling  
422 methods have the advantages of increasing sampling coverage and frequency, but they also introduce bias due to  
423 the pressure generated by high speeds, resulting in even greater undersampling compared to traditional nets (Harris  
424 et al., 2000; Cook and Hays, 2001).

### 425 3.2.1 Impact on filtered volumes estimation

426 One of the primary challenges in quantitative plankton sampling is the estimation of the filtered volume. Because  
427 the immersion depth of surface nets changes constantly with waves, wind and boat movement, it is difficult to  
428 accurately calculate the volume of water being filtered (reviewed in Pasquier et al., 2022). Results obtained by  
429 different studies show that a surface sampling with a difference in immersion depth of a few centimeters can lead  
430 to a large difference in the sampled volume (Pasquier et al., 2022). Overall, the impact of high-speed deployment  
431 on filtered volume remains largely unexplored in the literature with the exception of Jonas et al (2004). They  
432 tested the relationship between CPR filtered volumes estimated by a flowmeter or by theory, and their relationship  
433 to CPR deployment speed. Their findings revealed overestimations by the flowmeter compared to theoretical  
434 values. This raises concerns about the effectiveness of flowmeters in measuring volumes during high-speed  
435 deployments. We therefore investigated whether our high-speed surface sampling approach had an effect on  
436 filtered volume measurements.

437  
438 For the Deck Net, the water intake was identical in design and mouth opening to HSN but a flowmeter was  
439 integrated into the water circuit downstream of the pump as well as two de-bubblers (pictures Fig. 6 in Gorsky et  
440 al., 2019). This allowed for reliable estimation of water volumes that were pumped into the Deck-net based on  
441 flowmeter recordings (Gorsky et al., 2019). Both HSN and Manta nets were equipped with mechanical flowmeters  
442 mounted in the inlet frame, while the towed distance, time and speed were recorded on board to also estimate the  
443 theoretical volume filtered. While the HSN was towed between 3.9 and 9 knots, the Manta net was towed at lower  
444 speed, between 1.2 knots and maximum speed of 3.6 knots (Fig. 6).

445



446



447  
448 **Figure 6. (a) and (b) Linear regression between volumes filtered estimated from the tow distance (theoric volumes; m3)**  
449 **and estimated from the flowmeters respectively for the HSN and Manta. The range of 95% confidence intervals is**  
450 **represented in orange for the HSN and in blue for the Manta. The 1:1 dotted line represents the linear regression**  
451 **obtained if both volumes were similar. The colour of the dots represents the deployment speed of the net in knots.**

452  
453 Figure 6 shows clear discrepancies in the slope of the estimated volumes between the HSN and the Manta,  
454 meaning that the theoretical and flowmeter filtered volumes of the Manta are closer to each other than for the  
455 HSN. Manta theoretical volumes tend to be higher and thus potentially overestimated compared to flowmeter  
456 measurements (Fig. 6b), but the difference remains largely small compared to the HSN. For this one, flowmeter  
457 estimation methods provide volumes in the same order of magnitude as the theoretical volume for HSN, yet exhibit  
458 considerable differences between stations (mean difference between flowmeter and theoretical volumes per station  
459 = 90.5, standard deviation = 172.6; Fig. 6a). Linear regression analysis between this volume differences per station  
460 (flowmeters - theoretical volume) and speed deployment showed a significant relationship with a slope coefficient  
461 of 91.168 (standard deviation = 11.86, t-test = 7.69 and p-value < 0.001), indicating that higher speeds are  
462 associated with greater differences. Consistently with the results of Jonas et al (2004) described before, the high-  
463 speed deployment is thus associated with the overestimation of the flowmeters volumes compared to theoretical  
464 ones (Fig. 6a). These results indicate that the use of the flowmeters is not appropriate in high-speed conditions.  
465 The pressure increase caused by the high speed generates turbulence, could affect the flowmeter rotation and  
466 explain the overestimation of the filtered volume for the high-speed that we found. Globally, the turbulence  
467 generated could explain the malfunction of flowmeters which are designed and calibrated by the manufactures to  
468 accurately measure flow speed in a laminar flow. This result is highlighted by Skjoldal et al. (2019), who assume  
469 the use of flowmeters being complex because of their position in relation to the cross-sectional flow field or  
470 functioning in a turbulent system.

471  
472 In addition to the speed, we tested the HSN's immersion depth varied when the sea state was high. The HSN was  
473 designed to sample the surface ocean, at the air-seawater interface, thus the upper part of its mouth opening was  
474 rarely completely submerged during the deployment (see images Fig. 4 in Gorsky et al. 2019). The relationships  
475 between wind strength (as a proxy for sea state) recorded by Tara's navigation instruments and the two estimates  
476 of HSN sampling volumes showed no correlation ( $R^2 = 0.00$  for flowmeter volumes and for theoretical volumes;  
477 data not shown). While the flowmeter does not provide accurate flow measurements under turbulent conditions,  
478 it appears that the sea state does not affect its volume estimates.

479  
480 Therefore, we recommended using the theoretical volume for the HSN. The towing distance used is relative to  
481 ground, not to the seawater, therefore there is a potential bias in the theoretical volume estimation due to the non-  
482 consideration of the surface current speed. This bias is likely negligible for the majority of our samples located in  
483 the subtropical gyres, mostly characterised by relatively low geostrophic currents (Tara Pacific data available  
484 Bourdin et al. 2022 in 'at current\_speed\_copernicus').

485

### 486 3.2.2 Quantitative comparison between HSN and Manta

487 The Manta net is the most commonly used net for studying surface plankton, widely recognised as a reference  
488 system for investigating surface ocean (Eriksen et al., 2018; Karlsson et al., 2020; Pasquier et al, 2022). Both HSN  
489 and Manta nets were deployed at the same stations when approaching islands and in the Great Pacific Garbage  
490 Patch. The Manta net was deployed in closer proximity to islands than the HSN net. Given that the HSN net was  
491 towed for a duration of 60–90 minutes, while the Manta net was towed for approximately 30–40 minutes, the  
492 decision was taken to sample with the Manta net in the immediate vicinity of the island, in order to capture the  
493 variability associated with the island mass effect.

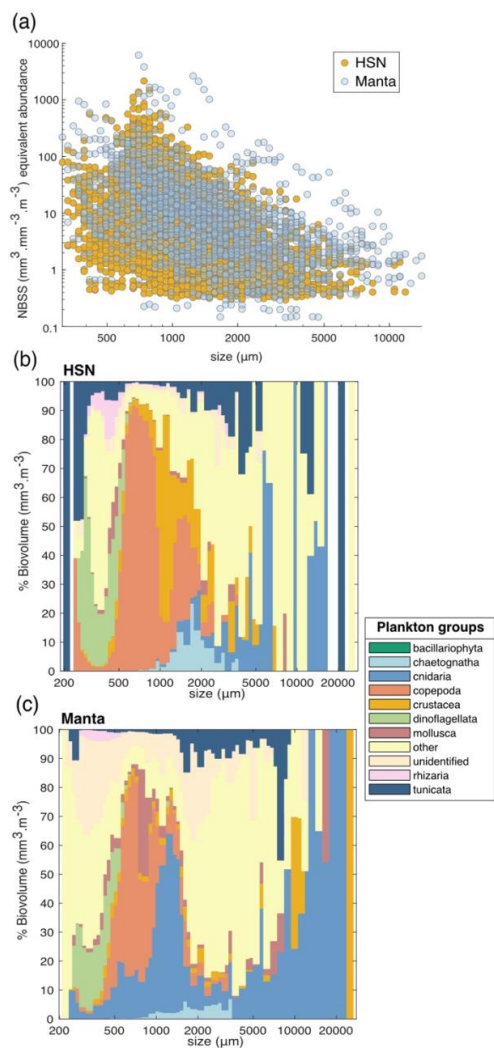
494

495 We conducted a comparison of the Normalized Biovolume Size Spectra (NBSS; Fig. 7a) obtained from the two  
496 nets. The analysis follows the analysis presented in Lombard et al. (2023), incorporating data from 31 additional





497 samples collected by the HSN. Abundances based on the NBSS of both nets were on the same order of magnitude  
 498 with Manta abundances appearing higher (Fig. 7a). This difference was expected due to the undersampling at high  
 499 speed compared to traditional plankton sampling discussed above. In contrast to the HSN net, which has a smaller  
 500 mouth opening leading to a smaller sampling volume, the Manta net benefits from a larger opening and lower  
 501 towing speed. This combination reduces turbulence and allows for a larger sampling volume, resulting in  
 502 potentially lower loss. This is reflected in Fig. 7a, where the Manta net captures a wider range of sizes, including  
 503 larger and rarer fragile organisms. Skjoldal et al. (2019) measured less biomass in the large size fraction and more  
 504 biomass in the small and medium size fractions at the higher towing speeds. The opposite effect might have been  
 505 expected for the small fraction due to extrusion (Skjoldal et al., 2019). Assuming the same water masses were  
 506 sampled, the HSN net appears to be more effective at capturing smaller organisms, as indicated by the fact that  
 507 the slopes of the HSN's equivalent abundance is steeper than the Manta's (mean NBSS slope for HSN = -0.35, std  
 508 = 0.30 and mean NBSS slope for Manta = -0.30, std = 0.23; Fig. 7a).  
 509



510  
 511



512 **Figure 7. (a) Comparison of Normalized Biovolume Size Spectra (NBSS) of living organisms sampled with HSN in**  
513 **yellow dots and Manta nets in blue dots. Only stations where both were deployed are included in this figure. Average**  
514 **taxonomic composition of the ‘plankton groups’ in biovolume ( $\text{mm}^3/\text{m}^3$ ) for all stations by size class (in  $\mu\text{m}$ ) for samples**  
515 **collected with HSN in (b) and Manta net in (c).**

516

517 All these observed differences may therefore introduce differences in species composition. Investigating the  
518 taxonomic composition, the HSN and the Manta show on average relatively similar community compositions  
519 (Fig. 7c and 7d). The dinoflagellates are almost entirely composed of the genus *Noctiluca*. As we discussed above,  
520 the HSN net undersampled larger and more fragile organisms like cnidarians and tunicates (Fig. 7c). This aligns  
521 with the limitations of high-speed deployments, which have been shown to damage delicate organisms (Harris et  
522 al., 2000; Keen, 2013). This damage to large and fragile plankton could cause the higher concentrations of smaller  
523 size classes we found in HSN compared to Manta samples. In contrast, the HSN consistently sampled more robust  
524 organisms such as copepods and chaetognaths than the Manta (Fig. 7c and 6d).

525

526 Given that plankton concentrations are higher in the areas surrounding the islands (Bourdin et al., in rev) deploying  
527 the manta net closer to these islands could also affect the observed differences in plankton concentrations between  
528 the two nets. In conclusion, the use of the HSN introduces an undersampling bias that is also found in other high-  
529 speed samplers, as described for the CPR. The HSN must therefore be considered as semi-quantitative.  
530 Nevertheless, we highlight the usefulness of the HSN for sampling surface zooplankton when it is not possible to  
531 stop or slow the boat, and its value in extending sampling coverage and frequency. Consistent with the CPR  
532 conclusion, HSN captures a roughly consistent fraction of the in-situ abundance reflecting the main patterns  
533 observed in plankton. For example, the trend of increasing plankton abundance due to Californian upwelling  
534 (Checkley and Barth, 2009) appears to emerge regardless of the sampling method used (see Fig. B1 to B4,  
535 appendix B). Each net is a filter through which we sample the ocean, but if the overall patterns they show are  
536 consistent, we can conclude that they are likely to be robust patterns. This is true for many types of sampling nets,  
537 as many previous studies have shown (Herdman, 1921; Barnes and Marshall, 1951; Anraku, 1956; Wiebe and  
538 Holland, 1968).

### 539 **Conclusion**

540 The Tara Pacific Expedition introduces, to our knowledge, the first system adapted for discrete sampling of the  
541 whole, end-to-end, planktonic ecosystem, from viruses to metazoa, deployed and recovered at cruising speed (5–  
542 9 knots). Our observations on these two new sampling systems highlight biases, particularly the under-sampling  
543 of fragile organisms (e.g., gelatinous plankton), which is important to consider in subsequent ecological analyses.  
544 However, high-speed sampling provides valuable opportunities to expand the coverage and frequency of plankton  
545 collection, helping to address the critical issue of under-sampling in the open ocean, a major challenge for global  
546 plankton research. This has provided an adaptable framework for studying planktonic ecosystems at spatial and  
547 temporal scales that are difficult to achieve. These systems can also be easily adapted to vessels of various sizes  
548 and propulsion systems, paving the way for complementary initiatives, such as plankton collection by citizen  
549 sailors (De Vargas et al., 2022; Mériguet et al., 2022).

550

551 In conclusion, with these innovative methods, we provide an important dataset covering nearly the whole Pacific  
552 Ocean and North Atlantic one, and focusing on the surface plankton which is rarely sampled as a whole, but rather  
553 focused on the plastic and large neustonic inhabitants. Such a large dataset, consistently sampled, at a large scale  
554 open the way to further studies focusing on how different environmental imprints (Lombard et al., 2023) may  
555 affect this particular ecosystem, from large scale to mesoscale levels, and how these observations may relate to  
556 other types of observations from species barcodes to genomes (Besler et al., 2023). Such important dataset will,  
557 without doubt, not only serves as a starting point for many studies to deepen our understanding of planktonic  
558 ecosystems, their biogeochemical roles, and their socio-economic importance, but could serves as a reference state  
559 of the ecosystem in the context of environmental changes.



560 **4. Data availability**

561 The referenced datasets related to figures are available at:  
 562 <https://doi.org/10.17882/102537> Mériguet et al., (2024a),  
 563 <https://doi.org/10.17882/102336> Mériguet et al., (2024b),  
 564 <https://doi.org/10.17882/102694> Mériguet et al., (2024c)  
 565 and <https://doi.org/10.17882/102697> Mériguet et al., (2024d).

566 The datasets are also summarized in Table 2.

567  
 568  
 569

	Datasets			
Name	FlowCam Tara Pacific DN 20 microns	FlowCam Tara Pacific Bongo 20 microns	ZooScan Tara Pacific HSN 330 microns	ZooScan Tara Pacific Manta 333 microns
DOI	10.17882/102697	10.17882/102694	10.17882/102336	10.17882/102537
Sampling Location	Open-ocean and islands sampling	Islands, reef and lagoon sampling	Open-ocean and islands sampling	Open-ocean (Great Pacific Garbage Patch) and islands sampling
Plankton size imaged	(20-200 µm)	(20-200 µm)	(> 300 µm)	(> 300 µm)
Link to open EcoTaxa project	Subset 30% < 500 pixels: <a href="https://ecotaxa.obs-vlfr.fr/prj/11353">https://ecotaxa.obs-vlfr.fr/prj/11353</a>	Subset 30% < 500 pixels: <a href="https://ecotaxa.obs-vlfr.fr/prj/11370">https://ecotaxa.obs-vlfr.fr/prj/11370</a>	<a href="https://ecotaxa.obs-vlfr.fr/prj/11292">https://ecotaxa.obs-vlfr.fr/prj/11292</a>	Subset Plankton images <a href="https://ecotaxa.obs-vlfr.fr/prj/1344">https://ecotaxa.obs-vlfr.fr/prj/1344</a>
	Subset 100 % > 501 pixels: <a href="https://ecotaxa.obs-vlfr.fr/prj/11341">https://ecotaxa.obs-vlfr.fr/prj/11341</a>	Subset 100 % > 501 pixels: <a href="https://ecotaxa.obs-vlfr.fr/prj/11369">https://ecotaxa.obs-vlfr.fr/prj/11369</a>		Subset Plastics images <a href="https://ecotaxa.obs-vlfr.fr/prj/1345">https://ecotaxa.obs-vlfr.fr/prj/1345</a>
	Export EcoTaxa FlowCam Tara Pacific DN 20 microns < 500 pixels.zip	Export EcoTaxa FlowCam Tara Pacific Bongo 20 microns < 500 pixels.zip		Export EcoTaxa ZooScan Tara Pacific HSN 330 microns.zip
ZIP files with one tsv per samples, raw export from EcoTaxa	Subset 100 % > 501 pixels: Export EcoTaxa FlowCam Tara Pacific DN 20 microns > 501 pixels.zip	Subset 100 % > 501 pixels: Export EcoTaxa FlowCam Tara Pacific Bongo 20 microns > 501 pixels.zip		Subset Plastics images Export EcoTaxa ZooScan Tara Pacific Manta 333 microns plastics.zip



<b>CSV files with ab, bv (x3: area, riddled and ellispoidal), shannon</b>	Descriptors FlowCam Tara Pacific DN 20 microns.csv	Descriptors FlowCam Tara Pacific Bongo 20 microns.csv	Descriptors ZooScan Tara Pacific HSN 330 microns.csv	Descriptors ZooScan Tara Pacific Manta 333 microns.csv
<b>ZIP files with 1 table csv / sample for NBSS (1 NBSS / sample)</b>	NBSS FlowCam Tara Pacific DN 20 microns.zip	NBSS FlowCam Tara Pacific Bongo 20 microns.zip	NBSS ZooScan Tara Pacific HSN 330 microns.zip	NBSS ZooScan Tara Pacific Manta 333 microns.zip

570

571 **Table 2. Summary of data availability, description and useful link for each dataset.**

572 **Appendices**

573

<b>FlowCam Tara Pacific DN 20 microns</b>		
Taxonomic list	Plankton groups	Trophic type
Bacillariophyceae	bacillariophyta	phototroph
Asterionellopsis		
Asterolamprales		
Bacillariaceae		
Climacodium		
Climacodium inter. Crocosphaera		
chainlarge		
chainthin		
multiple < Diatoma		
Pseudo-Nitzschia chain		
Thalassionematales		
Corethron		
Coscinodiscophycidae		
Coscinodiscids		
Bacteriastrum		
Chaetoceros		
Chaetoceros protuberans		
Chaetoceros peruvianus		
Ditylum		
Eucampia		
Hemiaulus		
Fragilariopsis		
Nitzschia		
Planktoniella sol		
Rhizosolenids		



Dactyliosolen		
Guinardia		
Rhizosolenia inter. Richelia		
pennate < Bacillariophyta		
Helicotheca		
Cyanobacteria	cyanobacteria	autotroph
UCYNA like		
cyano a		
cyano b		
Richelia		
attached		
Codonaria	ciliophora	mixotroph
Ciliophora		
Amphorides		
Codonellidae		
Codonellopsis		
Codonellopsis orthoceras		
Cyttarocylis		
Dictyocysta		
Epiplocylis		
Eutintinnus		
Lacrymaria		
Metacylis		
Poroecus		
Rhabdonella		
Rhabdonellopsis		
Salpingella		
Steenstrupiella		
Tintinnida		
Undellidae		
Amplectella		
Xystonellidae		
Dadayiella		
Zoothamniidae		
Dictyochophyceae	dictyochophyceae	phototroph
Gonyaulacales	dinoflagellata	mixotroph
Dinophyceae		
Amphisolenia		
Dinophysis		



Ceratocorys		
Cladopyxis		
Neoceratium		
Neoceratium limulus		
Neoceratium candelabrum		
Neoceratium furca		
Neoceratium fusus		
Neoceratium pentagonum		
Neoceratium geniculatum		
Pyrocystaceae		
Pyrophacus		
Gymnodiniales		
Ornithocercus		
Ornithocercus heteroporus		
Ornithocercus magnificus		
Ornithocercus quadratus		
Ornithocercus steinii		
Oxytoxum		
Phalacroma		
Podolampas		
Protoperidinium		
polar view		
Hemidiscus cuneiformis		
Tunicata	tunicata	grazers
Appendicularia		
Copepoda	copepoda	
Ostracoda	crustacea	
nauplii < Crustacea		
Rotifera	other	
trochozoa		
larvae < Annelida		omnivorous
veliger	mollusca	grazers
Pterosperma	other	phototroph
Rhizaria	rhizaria	mixotroph
Retaria		
Amphibelone		
Acantharia		
Foraminifera		
Nassellaria		



Spumellaria		
cyst	other	–
egg		
egg sac		
multiple < other	–	–
othertocheck	other unidentified	unidentified
darkrods < othertocheck		
lightrods < othertocheck		
othersphere		
t001	other unidentified	unidentified
t003		
t004		
tail < Appendicularia	non-living	–
part < Crustacea		
spines < Acantharea		
part < Ciliophora		
artefact		
badfocus < artefact		
bubble		
detritus		
dark < detritus		
fiber < detritus		
light < detritus		
pollen		
duplicate		
t002		

574  
 575  
 576

**Table A1. List of EcoTaxa taxonomic annotations and associated groups: plankton groups and trophic type for the FlowCam DN 20 microns dataset.**

FlowCam Tara Pacific Bongo 20 microns		
Taxonomic list	Plankton groups	Trophic type
Trichodesmium	cyanobacteria	autotroph
UCYNA like		
Cyanobacteria<Proteobacteria		
Richelia		
Ciliophora	ciliophora	mixotroph



Lacrymaria<Lacrymariidae		
Vorticella		
Codonellidae		
Cyttarocyliis		
Epiplocyliis		
Dictyocysta		
Metacyliis		
Rhabdonella		
Rhabdonellopsii		
Tintinnida		
tintinnid-diatom		
Amphorides<Tintinnidiidae		
Eutintinnus		
Salpingella<Tintinnidiidae		
Steenstrupiella		
Tintinnidae X		
Poroecus		
Undellidae		
Xystonellidae		
part<Ciliophora		
Dinophyceae		
Dinophyceae X		
Amphisolenia		
Ornithocercus		
Ornithocercus magnificus<Ornithocercus		
Ornithocercus steinii		
Phalacroma		
Neoceratium		
Neoceratium candelabrum		
Neoceratium furca<Neoceratium	dinoflagellata	mixotroph
Neoceratium fusus<Neoceratium		
Neoceratium pentagonum		
Cladopyxis		
Ostreopsis		
Pyrocystaceae		
Pyrophacus		
Peridinales		
Oxytoxum		
Podolampas		
Protoperidinium		





Rhizaria	rhizaria	mixotroph
Retaria		
Acantharea		
spines<Acantharea		
Foraminifera		
Nassellaria<Polycystinea		
Spumellaria		
Radiolaria		
aggregate<Radiolaria		
part<Rhizaria		
spines<Rhizaria		
Bacillariophyceae	bacillariophyta	phototroph
Asterionella		
Coccinodiscophycidae		
Asterolamprales		
Hemidiscus cuneiformis		
Hemidiscus		
Cylindrotheca		
Diatoma		
chainlarge		
chainthin		
multiple<Diatoma		
Licmophora		
Naviculales		
Nitzschia		
Pseudo-nitzschia		
Striatella		
Synedra		
Thalassionematales		
Amphitetras		
Bacteriastrum<Mediophyceae		
Biddulphia		
Chaetoceros<Mediophyceae		
Chaetoceros inter ciliate		
Chaetoceros inter. Calothrix		
Ditylum		
Eucampia		
Hemiaulus		
Odontella sp.		



Odontella<Mediophyceae		
Planktoniella		
Corethron		
Coscinodiscus		
Stephanopyxis		
Rhizosolenids		
Dactyliosolen		
Guinardia		
Rhizosolenia		
Rhizosolenia inter. Richelia		
rhizosolenia inter richelia tmp i		
rhizosolenia tmp i		
centric		
chain<centric		
pennate<Bacillariophyta		
part diatom		
Dictyochophyceae		
Dictyochales	dictyochophyceae	phototroph
Dictyocha		
Annelida		
larvae<Polychaeta	others	grazers
trocophora		
larvae<Annelida		
trochophore		
Copepoda<Maxillopoda		
Calanoida	copepoda	omnivorous
Cyclopoida		
Oithonidae		
Harpacticoida		
Corycaeidae		
Oncaeidae		
part<Copepoda		
nauplii<Crustacea	crustacea	grazers
part<Crustacea		
Bryozoa	other	grazers
trochozoa		



larvae<Echinodermata		
Mollusca	mollusca	
veliger		
larvae<living	other	unidentified
other<living		
egg<other		–
egg sac<egg		
multiple<other	–	–
duplicate		
othertocheck	other unidentified	unidentified
crumple sphere		
darkrods<othertocheck		
lightrods<othertocheck		
t001	other unidentified	unidentified
t002		
t003		
t004		
t005		
t006		
t007		
t008		
t010		
t011		
t012		
t013		
t014		
t015		
t016		
t017		
part<other	non-living	–
part<seaweed		
Micracanthodinium quadrispinum		
artefact		
badfocus<artefact		
bubble		
detritus		



aggregates		
dark<detritus		
fiber<detritus		
light<detritus		
feces		
darkrods<rods		
lightrods<rods		

577

578 **Table A2. List of EcoTaxa taxonomic annotations and associated groups: plankton groups and trophic type for the**  
 579 **FlowCam Bongo 20 microns dataset.**

ZooScan Tara Pacific HSN 330 microns		
Taxonomic list	Plankton groups	Trophic type
Actinopterygii	other	predators
egg < Actinopterygii		
Annelida	other	omnivorous
Spirorbis		
larvae < Annelida		
Appendicularia	tunicata	grazers
Oikopleuridae		
Bryozoa	other	grazers
cyphonaute		
Chaetognatha	chaetognatha	predators
Hydrozoa	cnidaria	predators
Scyphozoa		
Porpita		
larvae < Porpitiidae		
Siphonophorae		
bract < Abylidae		
gonophore < Abylidae		
nectophore < Abylidae		
Diphyidae		
bract < Diphyidae		
eudoxie < Diphyidae		
gonophore < Diphyidae		
nectophore < Diphyidae		
nectophore < Hippopodiidae		



Abylopsis tetragona		
bract < Abylopsis tetragona		
eudoxie < Abylopsis tetragona		
gonophore < Abylopsis tetragona		
nectophore < Abylopsis tetragona		
bract < Bassia bassensis		
nectophore < Bassia bassensis		
Physonectae		
nectophore < Physonectae		
Verella		
polype < Leptothecata		
polype < Anthozoa		
Cirripedia	crustacea	grazers
cirrus		
cypris		
nauplii < Cirripedia		
Evadne		
Podon		
Calanoida	copepoda	omnivorous
Acartiidae		
Calanidae		
Calocalanus pavo		
Candaciidae		
Centropagidae		
Eucalanidae		
Euchaetidae		
Heterorhabdidae		
Metridinidae		
Pontellidae		
Pontellina plumata		
Monstrilloida		
Temoridae		
Oithonidae		
Harpacticoida		
Corycaeidae		
Oncaeidae		
Sapphirinidae		
Copilia		
Lubbockia		



Siphonostomatoida		
badfocus < Copepoda		
damaged < Copepoda		
multiple < Copepoda		
Crustacea	crustacea	predators
Eumalacostraca		
Amphipoda		
Caprellidae		
Gammaridea		
protozoa		
Hyperidea		
Brachyura		
Phronimidae		
megalopa		
zoa < megalopa		
Euphausiacea		
calyptopsis < Euphausiacea		
Isopoda		
Laomediidae		
larvae < Porcellanidae		
phyllosoma		
nauplii < Crustacea	crustacea	grazers
metanauplii < Crustacea		
Ostracoda		
larvae < Squillidae		
Cyanobacteria < Bacteria	cyanobacteria	autotroph
Echinodermata	other	grazers
echinopluteus		
pluteus < echinoidea		
ophiuroida		
ophiopluteus		
pluteus<ophiuroida		
Harosa	rhizaria	mixotroph
Acantharia		
Collodaria		
Globorotalidae		



Orbunila		
Foraminifera		
Spumellaria		
Pyrocystaceae	dinoflagellata	mixotroph
multiple < Pyrocystaceae		
Insecta	other	predators
Halobates		
Mollusca	mollusca	grazers
Bivalva		
Gymnosomata		
Cavolinia inflexa		
Diacria		
Atlanta		
Cavoliniidae		
Cephalopoda		
Creseidae		
Creseis acicula		
Creseis virgula		
Firola		
Limacinidae		
part < Mollusca		
veliger		
Doliolida	tunicata	predators
Salpida		
juvenil < Salpida		
nucleus < Salpida		
egg < other	other	-
egg sac < egg		
gelatinous	other	predators
nudibranchia	other	-
multiple < other	other	-
othertocheck	other unidentified	unidentified



darksphere		
othersphere		
t001	other unidentified	unidentified
t002		
t003		
t004		
part < Actinopterygii	non-living	-
scale < Actinopterygii		
trunk < Appendicularia		
head < Chaetognatha		
part < Annelida		
tail < Appendicularia		
tail < Chaetognatha		
part < Thaliacea		
part < Siphonophorae		
part < Copepoda		
part < Cnidaria		
part < Crustacea		
part < Ctenophora		
wing < Halobates		
empty < Ostracoda		
artefact		
badfocus < artefact		
bubble		
detritus		
borax		
dark < detritus		
fiber < detritus		

580

581 **Table A3. List of EcoTaxa taxonomic annotations and associated groups: plankton groups and trophic type for the**  
 582 **ZooScan HSN 330 microns dataset.**

583

Tara Pacific 2016 2018 Manta 300 plankton		
Taxonomic list	Plankton groups	Trophic type
Actinopterygii	other	predators
egg < Actinopterygii		
Annelida	other	omnivorous
larvae < Annelida		





Alciopidae		
Tomopteridae		
Spirorbis		
Terebellidae		
Fritillariidae	tunicata	grazers
Oikopleuridae		
Chaetognatha	chaetognatha	predators
Cnidaria		
polype < Anthozoa		
Hydrozoa		
larvae < Porpitidae		
Porpita porpita		
Velella		
polype < Leptothecata		
bract < Abylopsis tetragona		
eudoxie < Abylopsis tetragona		
gonophore < Abylopsis tetragona		
nectophore < Abylopsis tetragona		
bract < Bassia bassensis		
gonophore < Bassia bassensis		
nectophore < Bassia bassensis		
bract < Diphyidae		
Chelophyes		
eudoxie < Diphyidae		
eudoxie < Eudoxoides spiralis		
gonophore < Eudoxoides spiralis		
nectophore < Eudoxoides spiralis		
gonophore < Diphyidae		
nectophore < Diphyidae		
nectophore < Hippopodiidae		
Physalia		
nectophore < Physonectae		
Aglaura		
Rhopalonema velatum		
ephyra		
Ctenophora	other	predators



cirrus	crustacea	grazers
cypris		
nauplii < Cirripedia		
Evadne		
larvae < Crustacea		
metanauplii < Crustacea		
Eumalacostraca	crustacea	predators
Amphipoda		
Gammaridea		
Hyperiidea		
Oxycephalidae		
Phronima		
protozoa < Penaeidae		
protozoa < Sergestidae		
zoea < Galatheidae		
larvae < Porcellanidae		
Brachyura		
megalopa		
zoea < Brachyura		
like < Laomediidae		
calyptopsis		
protozoa < Mysida		
Crustacea	crustacea	predators
nauplii < Crustacea		
metanauplii < Crustacea		
Ostracoda		
larvae < Squillidae		grazers
Copepoda	copepoda	omnivorous
Calanoida		
Acartiidae		
Haloptilus		
Calanidae		
Candaciidae		
Centropagidae		
Eucalanidae		
Euchaetidae		
Metridinidae		
Calocalanus pavo		



Pontellidae		
Pontellina plumata		
Temoridae		
Oithonidae		
Harpacticoida		
Miraciidae		
Corycaeidae		
Lubbockia		
Oncaeidae		
Sapphirinidae		
Copilia		
badfocus < Copepoda		
multiple < Copepoda		
damaged < Copepoda		
Insecta	other	predators
Gerridae		
Bryozoa	other	grazers
cyphonaute		
Branchiostoma lanceolatum	other	grazers
Doliolida		
Pyrosomatida		
Salpida	tunicata	omnivorous
chain < Salpida		
juvenile < Salpida		
Mollusca		
Bivalvia		
Cephalopoda		
Atlanta		
Firola		
Gymnosomata		
Cavoliniidae	mollusca	grazers
Diacavolinia		
Diacria trispinosa		
Creseidae		
Creseis acicula		
Creseis virgula		



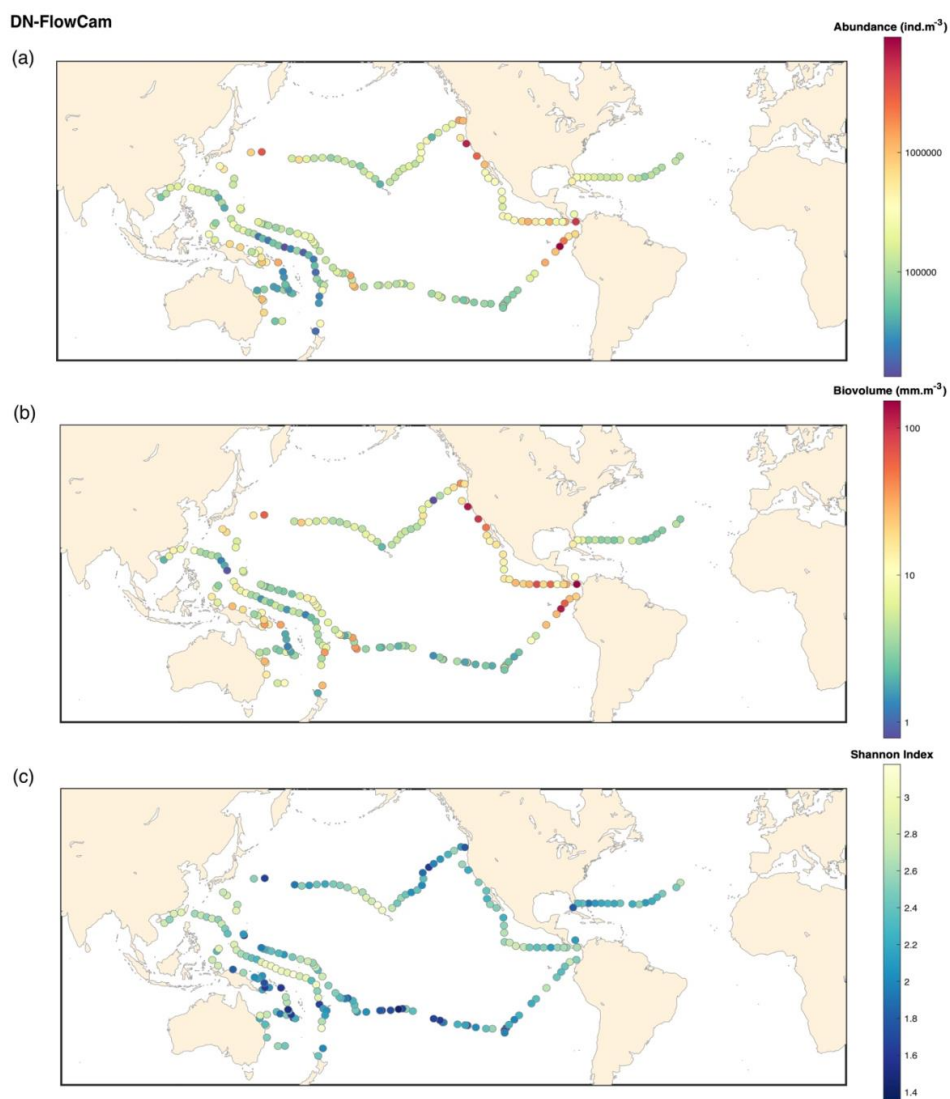
Limacinidae		
Nudibranchia		
egg < Mollusca	other	–
pluteus < Echinoidea	other	omnivorous
pluteus < Ophiuroidea		
Harosa	other	mixotroph
Neoceratium	dinoflagellata	
Pyrocystaceae		
Foraminifera	rhizaria	
Orbulina		
Spumellaria		
Diatoma	diatoms	phototroph
egg < other	other	–
living < other	other	–
multiple < other	other	–
othertocheck	other unidentified	unidentified
seaweed	other	phototroph
t002	other unidentified	unidentified
t003		
t004		
t005		
t007		
t008		
t010		
t012		
t013		
t014		
t015		
t016		
t017		
plastic<fiber	plastics	–
plastic<filament		



plastic<film		
plastic<fragment		
plastic<multiple		
plastic<other		
plastic<pellet		
plastic<polystyrene		
part<Copepoda		
part<other		
scale<Actinopterygii		
part<Annelida		
tail<Appendicularia		
trunk<Appendicularia		
head<Chaetognatha		
tail<Chaetognatha		
part<Siphonophorae		
part<Cnidaria		
part<Ctenophora		
part<Crustacea	non-living	-
wing<Insecta		
part<Thaliacea		
nucleus<Salpida		
part<Mollusca		
detritus		
artefact		
badfocus<artefact		
bubble		
dark<detritus		
fiber<detritus		

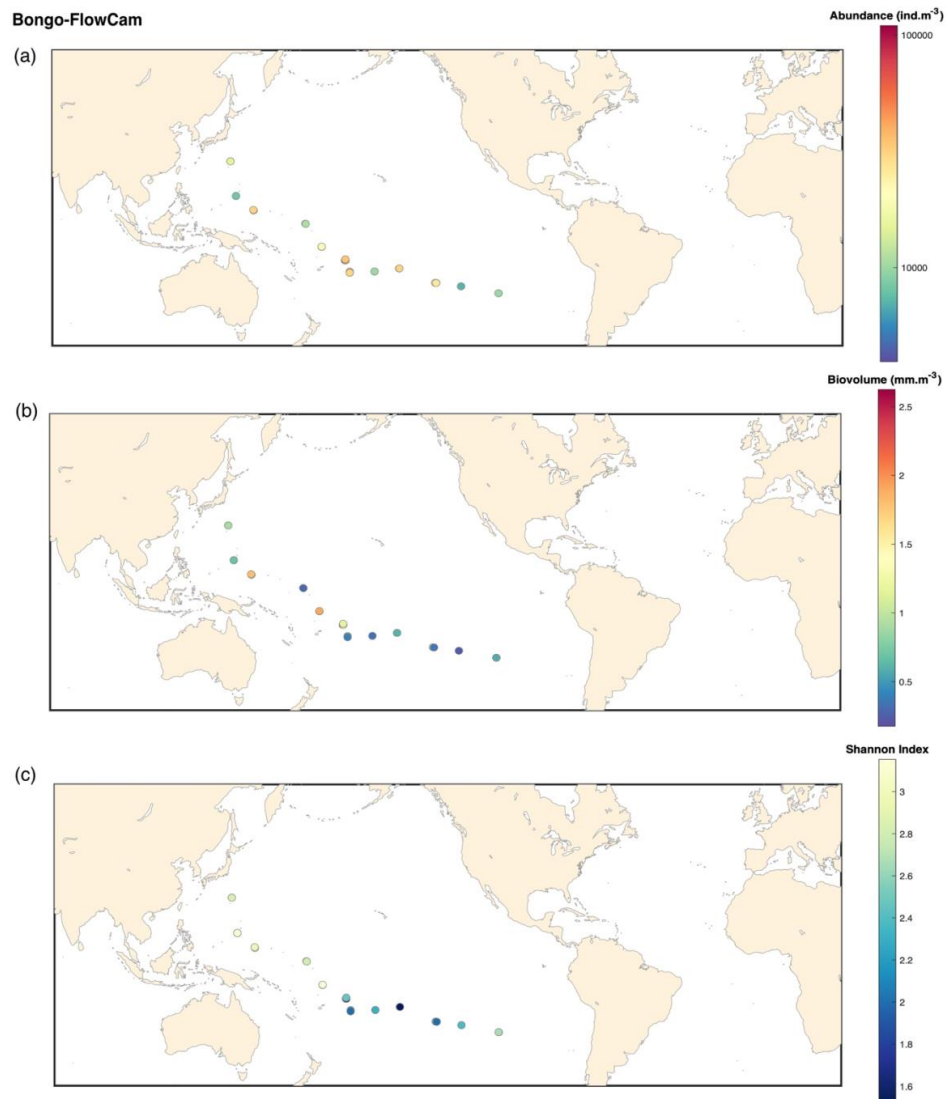
584

585 **Table A4. List of EcoTaxa taxonomic annotations and associated groups: plankton groups and trophic type for the**  
 586 **ZooScan Manta 333 microns dataset.**



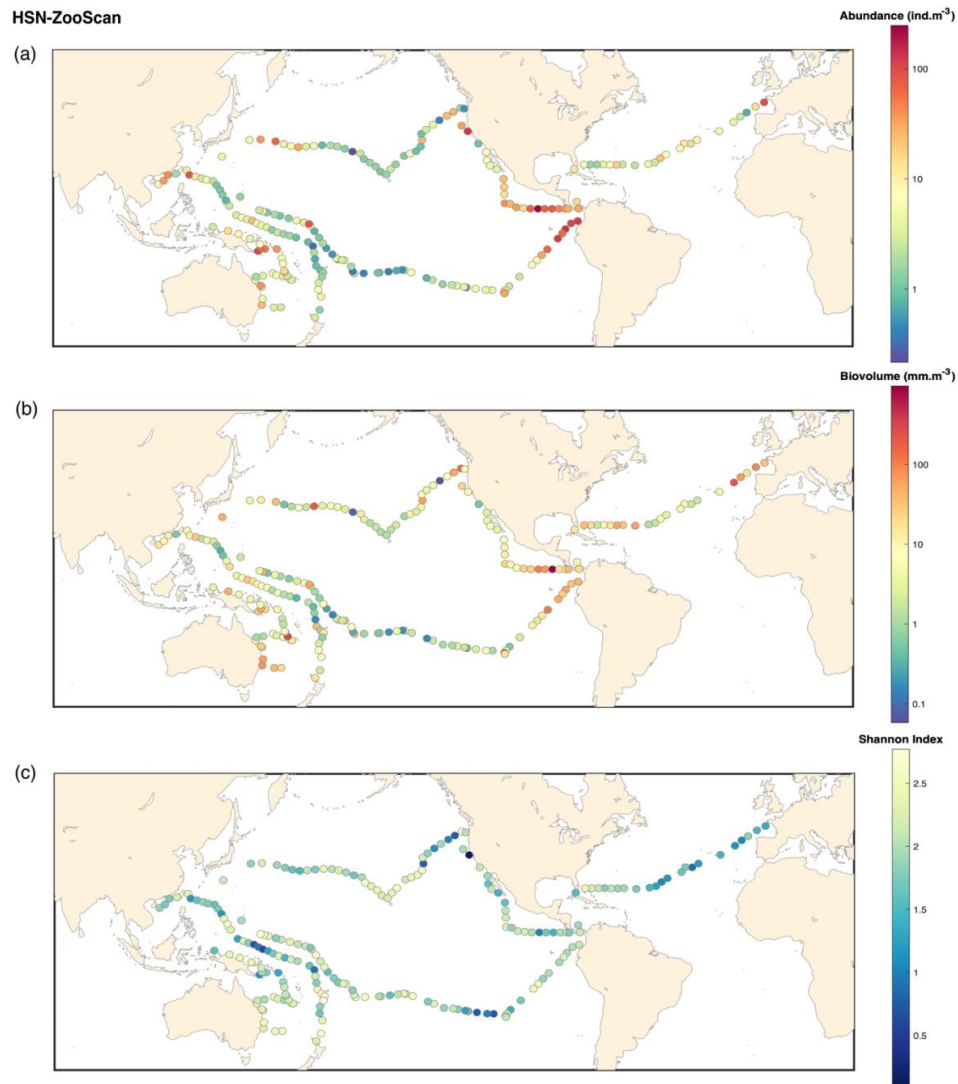
587  
588 **Figure B1. FlowCam DN 20 microns: (a) Map of plankton abundance (ind.m<sup>-3</sup>), (b) Map of plankton biovolume (mm.m<sup>-3</sup>), (c) Map of Shannon diversity Index.**  
589

590



591

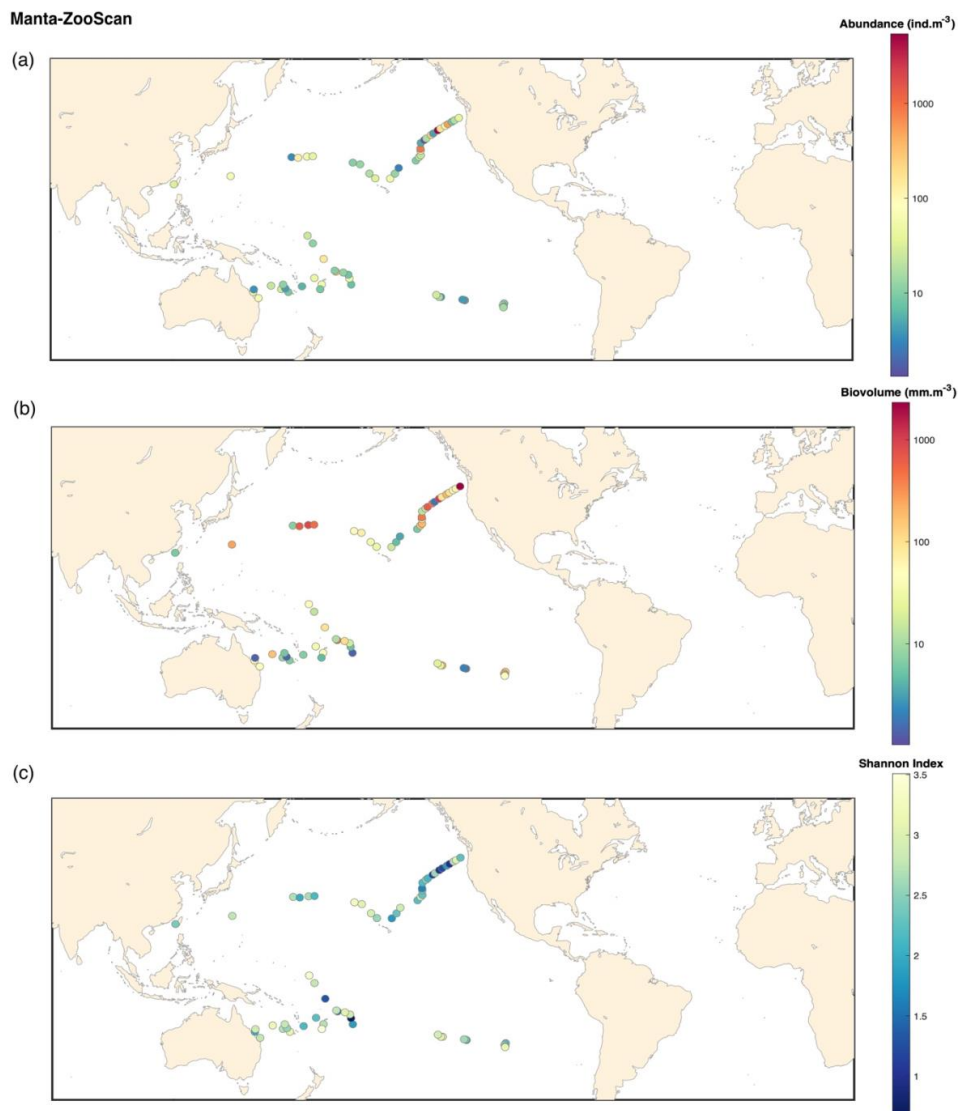
592 **Figure B2. FlowCam Bongo 20 microns: (a) Map of plankton abundance ( $\text{ind.m}^{-3}$ ). (b) Map of plankton biovolume**  
593 **( $\text{mm.m}^{-3}$ ). (c) Map of Shannon diversity Index.**



594  
595 **Figure B3. ZooScan HSN 330 microns: (a) Map of plankton abundance ( $\text{ind.m}^{-3}$ ). (b) Map of plankton biovolume**  
596 **( $\text{mm.m}^{-3}$ ). (c) Map of Shannon diversity Index.**

597





598 **Figure B4. ZooScan Manta 333 microns: (a) Map of plankton abundance (ind.m<sup>-3</sup>). (b) Map of plankton biovolume**  
599 **(mm.m<sup>-3</sup>). (c) Map of Shannon diversity Index.**  
600

601 **Team list**

602 Tara Pacific Consortium Coordinators:

603 Sylvain Agostini<sup>5</sup>, Denis Allemand<sup>6</sup>, Bernard Banaigs<sup>7</sup>, Emilie Boissin<sup>7</sup>, Emmanuel Boss<sup>3</sup>, Chris Bowler<sup>8</sup>,  
604 Colombar De Vargas<sup>9</sup>, Eric Douville<sup>10</sup>, Michel Flores<sup>11</sup>, Didier Forcioli<sup>12</sup>, Paola Furla<sup>12</sup>, Pierre Galand<sup>13</sup>, Eric  
605 Gilson<sup>14</sup>, Stéphane Pesant<sup>15</sup>, Serge Planes<sup>16</sup>, Stéphanie Reynaud<sup>17</sup>, Matthew B. Sullivan<sup>18</sup>, Shinichi Sunagawa<sup>19</sup>,  
606 Olivier Thomas<sup>20</sup>, Romain Troublé<sup>21</sup>, Rebecca Vega Thruher<sup>22</sup>, Christian R. Voolstra<sup>23</sup>, Patrick Wincker<sup>24</sup>, Didier  
607 Zoccola<sup>6</sup>  
608



- 609 <sup>5</sup>Shimoda Marine Research Center, University of Tsukuba, 5-10-1, Shimoda, Shizuoka, Japan  
610 <sup>6</sup>Centre Scientifique de Monaco, 8 Quai Antoine Ier, MC-98000, Principality of Monaco  
611 <sup>7</sup>PSL Research University: EPHE-UPVD-CNRS, USR 3278 CRIOBE, Université de Perpignan, France  
612 <sup>8</sup>Institut de Biologie de l'Ecole Normale Supérieure (IBENS), Ecole normale supérieure, CNRS, INSERM,  
613 Université PSL, 75005 Paris, France  
614 <sup>9</sup>Sorbonne Université, CNRS, Station Biologique de Roscoff, AD2M, UMR 7144, ECOMAP 29680 Roscoff,  
615 France  
616 <sup>10</sup>Laboratoire des Sciences du Climat et de l'Environnement, LSCE/IPSL, CEA-CNRS-UVSQ, Université Paris-  
617 Saclay, F-91191 Gif-sur-Yvette, France  
618 <sup>11</sup>Weizmann Institute of Science, Department of Earth and Planetary Sciences, 76100 Rehovot, Israel  
619 <sup>12</sup>Université Côte d'Azur, CNRS, INSERM, IRCAN, Medical School, Nice, France and Department of Medical  
620 Genetics, CHU of Nice, France  
621 <sup>13</sup>Sorbonne Université, CNRS, Laboratoire d'Ecogéochimie des Environnements Benthiques (LECOB),  
622 Observatoire Océanologique de Banyuls, 66650 Banyuls sur mer, France  
623 <sup>14</sup>Université Côte d'Azur, CNRS, Inserm, IRCAN, France  
624 <sup>15</sup>European Molecular Biology Laboratory, European Bioinformatics Institute, Wellcome Genome Campus,  
625 Hinxton, Cambridge CB10 1SD, UK  
626 <sup>16</sup>PSL Research University: EPHE-UPVD-CNRS, USR 3278 CRIOBE, Laboratoire d'Excellence CORAIL,  
627 Université de Perpignan, 52 Avenue Paul Alduy, 66860 Perpignan Cedex, France  
628 <sup>17</sup>Centre Scientifique de Monaco, 8 Quai Antoine Ier, MC-98000, Principality of Monaco  
629 <sup>18</sup>The Ohio State University, Departments of Microbiology and Civil, Environmental and Geodetic Engineering,  
630 Columbus, Ohio, 43210 USA  
631 <sup>19</sup>Department of Biology, Institute of Microbiology and Swiss Institute of Bioinformatics, Vladimir-Prelog-Weg  
632 4, ETH Zürich, CH-8093 Zürich, Switzerland  
633 <sup>20</sup>Marine Biodiscovery Laboratory, School of Chemistry and Ryan Institute, National University of Ireland,  
634 Galway, Ireland  
635 <sup>21</sup>Fondation Tara Océan, Base Tara, 8 rue de Prague, 75 012 Paris, France  
636 <sup>22</sup>Oregon State University, Department of Microbiology, 220 Nash Hall, 97331Corvallis OR USA  
637 <sup>23</sup>Department of Biology, University of Konstanz, 78457 Konstanz, Germany  
638 <sup>24</sup>Génomique Métabolique, Genoscope, Institut François Jacob, CEA, CNRS, Univ Evry, Université Paris-Saclay,  
639 91057 Evry, France

#### 640 **Author contribution**

641 Conceptualization and methodology: Tara Pacific Consortium; GB, GG, SA, DA, BB, EB, EB, CB, CDV, ED,  
642 MF, DF, PF, PG, EG, SP, SR, MBS, SS, OT, RT, RVT, CRV, PW, DZ, FL. Samples collection: GB, MLP, AE,  
643 GG. Samples analysis (on lab) and investigation: ZM, NK, LJ, OB, LC, JM, AE. Data analysis, curation and  
644 validation: ZM, NK, GB, LJ, MLP, MP, AE, LKB, FL. Supervision: GG, MLP, LKB, FL. Funding acquisition,  
645 project administration and resources: FL, GG, MLP, LKB, GB, SA, DA, BB, EB, EB, CB, CDV, ED, MF, DF,  
646 PF, PG, EG, SP, SR, MBS, SS, OT, RT, RVT, CRV, PW, DZ. Software: MP, ZM, GB, FL. Visualization and  
647 Writing – original draft preparation: ZM, GB, GG, FL, MP. All authors have read and reviewed the manuscript.

#### 648 **Competing interest**

649 The authors declare that they have no conflict of interest.

#### 650 **Acknowledgment**

651  
652 Special thanks to the Tara Ocean Foundation, the R/V Tara crew and the Tara Pacific Expedition Participants  
653 (<https://doi.org/10.5281/zenodo.3777760>). We are keen to thank the commitment of the following institutions for  
654 their financial and scientific support that made this unique Tara Pacific Expedition possible: CNRS, PSL, CSM,  
655 EPHE, Genoscope, CEA, Inserm, Université Côte d'Azur, ANR, agnès b., UNESCO-IOC, the Veolia Foundation,  
656 the Prince Albert II de Monaco Foundation, Région Bretagne, Billerudkorsnas, AmerisourceBergen Company,



657 Lorient Agglomération, Oceans by Disney, L'Oréal, Biotherm, France Collectivités, Fonds Français pour  
658 l'Environnement Mondial (FFEM), Etienne Bourgois, and the Tara Ocean Foundation teams. Tara Pacific would  
659 not exist without the continuous support of the participating institutes. The authors also particularly thank Serge  
660 Planes, Denis Allemand, and the Tara Pacific consortium. We thank the EMBRC collection CCPv for sample  
661 storage. This work was supported by EMBRC-France, whose French state funds are managed by the ANR within  
662 the Investments of the Future program under reference ANR-10-INBS-02. Support was also provided by the US  
663 National Science Foundation (NSF Biological Oceanography program (grant #2025402 to LKB) and the NASA  
664 Ocean Biology and Biogeochemistry program (grants #80NSSC20K1641). FL was also funded by the Institut  
665 Universitaire de France and co-funding by the European Union BIOcean5D GA#101059915 and the European  
666 Union's Horizon 2020 research and innovation programme "Atlantic Ecosystems Assessment, Forecasting and  
667 Sustainability" (AtlantECO) Grant ID: 862923. FL, OB, ZM are also funded by the ANR grant SmartBiodiv (grant  
668 ANR-21-AAFI-0002). This is publication number XX of the Tara Pacific Consortium. The authors particularly  
669 thank the Villefranche-sur-Mer Quantitative Imaging Platform (PIQv). Views and opinions expressed are however  
670 those of the author(s) only and do not necessarily reflect those of the European Union. Neither the European Union  
671 nor the granting authority can be held responsible for them.

## 672 References

- 673 Anraku, M.: Some experiments on the variability of horizontal plankton hauls and on the horizontal distribution  
674 of plankton in limited area. *Bull. Fat. Fisheries, Hokkaido Univ.*, 7: 1-16, 1956.
- 675 Barrows, A. P. W., Cathey, S. E., and Petersen, C. W.: Marine environment microfiber contamination: Global  
676 patterns and the diversity of microparticle origins, *Environmental Pollution*, 237, 275–284,  
677 <https://doi.org/10.1016/j.envpol.2018.02.062>, 2018.
- 678 Barnes, H. and Marshall, S. M.: On the variability of replicate plankton samples and some applications of  
679 "contagious" series to statistical distributions of catches over restricted periods, *J. mar. biol. Ass. U.K.*, 1951.
- 680 Bax, N. J., Miloslavich, P., Muller-Karger, F. E., Allain, V., Appeltans, W., Batten, S. D., Benedetti-Cecchi, L.,  
681 Buttigieg, P. L., Chiba, S., Costa, D. P., Duffy, J. E., Dunn, D. C., Johnson, C. R., Kudela, R. M., Obura, D.,  
682 Rebelo, L.-M., Shin, Y.-J., Simmons, S. E., and Tyack, P. L.: A Response to Scientific and Societal Needs for  
683 Marine Biological Observations, *Front. Mar. Sci.*, 6, 395, <https://doi.org/10.3389/fmars.2019.00395>, 2019.
- 684 Beaugrand, G.: Monitoring pelagic ecosystems using plankton indicators, *ICES Journal of Marine Science*, 62,  
685 333–338, <https://doi.org/10.1016/j.icesjms.2005.01.002>, 2005.
- 686 Belser, C., Poulain, J., Labadie, K., Gavory, F., Alberti, A., Guy, J., Carradec, Q., Cruaud, C., Da Silva, C.,  
687 Engelen, S., Mielle, P., Perdereau, A., Samson, G., Gas, S., Genoscope Technical Team, Batisse, J., Beluche, O.,  
688 Bertrand, L., Bohers, C., Bordelais, I., Brun, E., Dubois, M., Dumont, C., Zineb, E. H., Estrada, B., Ettedgui, E.,  
689 Fernandez, P., Garidi, S., Guérin, T., Gorrichon, K., Hamon, C., Kientzel, L., Lebled, S., Legrain, C., Lenoble,  
690 P., Lepretre, M., Louesse, C., Magdelenat, G., Mahieu, E., Martins, N., Milani, C., Orvain, C., Oztas, S., Payen,  
691 E., Petit, E., Rio, G., Robert, D., Ronsin, M., Vacherie, B., Voolstra, C. R., Galand, P. E., Flores, J. M., Hume, B.,  
692 C. C., Perna, G., Ziegler, M., Ruscheweyh, H.-J., Boissin, E., Romac, S., Bourdin, G., Iwankow, G., Moulin, C.,  
693 Paz García, D. A., Agostini, S., Banaigs, B., Boss, E., Bowler, C., De Vargas, C., Douville, E., Forcioli, D., Furla,  
694 P., Gilson, E., Lombard, F., Pesant, S., Reynaud, S., Sunagawa, S., Thomas, O. P., Troublé, R., Thurber, R. V.,  
695 Zoccola, D., Scarpelli, C., Jacoby, E. K., Oliveira, P. H., Aury, J.-M., Allemand, D., Planes, S., and Wincker, P.:  
696 Integrative omics framework for characterization of coral reef ecosystems from the Tara Pacific expedition, *Sci*  
697 *Data*, 10, 326, <https://doi.org/10.1038/s41597-023-02204-0>, 2023.
- 698 Bopp, L., Resplandy, L., Orr, J. C., Doney, S. C., Dunne, J. P., Gehlen, M., Halloran, P., Heinze, C., Ilyina, T.,  
699 Séférian, R., Tjiputra, J., and Vichi, M.: Multiple stressors of ocean ecosystems in the 21st century: projections  
700 with CMIP5 models, *Biogeosciences*, 10, 6225–6245, <https://doi.org/10.5194/bg-10-6225-2013>, 2013.
- 701 Borkman, D. G. and Smayda, T. J.: Gulf Stream position and winter NAO as drivers of long-term variations in  
702 the bloom phenology of the diatom *Skeletonema costatum* "species-complex" in Narragansett Bay, RI, USA,  
703 *Journal of Plankton Research*, 31, 1407–1425, <https://doi.org/10.1093/plankt/fbp072>, 2009.
- 704 Bourdin, G., Karp-Boss, L., Lombard, F., Gorsky, G., and Boss, E.: Dynamic island mass effect from space. Part  
705 I: detecting the extent, <https://doi.org/10.5194/egusphere-2024-2670>, 15 October 2024.



- 706 Bourdin, Lombard, Boss, Douville, Flores, Cassar, Cohen, Dimier, Fin, Gorsky, John, Kelly, Koren, Lin, Marie,  
707 MetzI, Pujo-Pay, Ras, Reverdin, Vardi, Conan, Ghiglione, Moulin, Boissin, Iwankow, Poulain, Romac, Agostini,  
708 Banaigs, Bowler, De Vargas, Forcioli, Furla, Galand, P. E., Gilson, E., Pesant, S., Reynaud, S., Sullivan, M. B.,  
709 Sunagawa, S., Thomas, O., Troublé, R., Vega Thurber, R., Voolstra, C. R., Wincker, P., Zoccola, D., Allemand,  
710 D., and Planes, S.: Environmental context observed during the Tara Pacific Expedition 2016-2018, simplified  
711 version at site level (1), <https://doi.org/10.5281/ZENODO.6474974>, 2022.
- 712 Chavez, F. P., Messié, M., and Pennington, J. T.: Marine Primary Production in Relation to Climate Variability  
713 and Change, *Annu. Rev. Mar. Sci.*, 3, 227–260, <https://doi.org/10.1146/annurev.marine.010908.163917>, 2011.
- 714 Checkley, D. M. and Barth, J. A.: Patterns and processes in the California Current System, *Progress in*  
715 *Oceanography*, 83, 49–64, <https://doi.org/10.1016/j.poccean.2009.07.028>, 2009.
- 716 Cook, K. B.: Comparison of the epipelagic zooplankton samples from a U-Tow and the traditional WP2 net,  
717 *Journal of Plankton Research*, 23, 953–962, <https://doi.org/10.1093/plankt/23.9.953>, 2001.
- 718 Copepod data base: <https://www.st.nmfs.noaa.gov/copepod/>, last access: 12 November 2024.
- 719 De Vargas, C., Le Bescot, N., Pollina, T., Henry, N., Romac, S., Colin, S., Haëntjens, N., Carmichael, M., Berger,  
720 C., Le Guen, D., Decelle, J., Mahé, F., Poulain, J., Malpot, E., Beaumont, C., Hardy, M., Guiffant, D., Probert, I.,  
721 Gruber, D. F., Allen, A. E., Gorsky, G., Follows, M. J., Pochon, X., Troublé, R., Cael, B. B., Lombard, F., Boss,  
722 E., Prakash, M., and the Plankton Planet core team: Plankton Planet: A frugal, cooperative measure of aquatic life  
723 at the planetary scale, *Front. Mar. Sci.*, 9, 936972, <https://doi.org/10.3389/fmars.2022.936972>, 2022.
- 724 Drago, L., Panaïotis, T., Irisson, J.-O., Babin, M., Biard, T., Carlotti, F., Coppola, L., Guidi, L., Hauss, H., Karp-  
725 Boss, L., Lombard, F., McDonnell, A. M. P., Picheral, M., Rogge, A., Waite, A. M., Stemmann, L., and Kiko, R.:  
726 Global Distribution of Zooplankton Biomass Estimated by In Situ Imaging and Machine Learning, *Front. Mar.*  
727 *Sci.*, 9, 894372, <https://doi.org/10.3389/fmars.2022.894372>, 2022.
- 728 Eriksen, M. B. and Frandsen, T. F.: The impact of patient, intervention, comparison, outcome (PICO) as a search  
729 strategy tool on literature search quality: a systematic review, *jmla*, 106, <https://doi.org/10.5195/jmla.2018.345>,  
730 2018.
- 731 Falkowski, P. G., Fenchel, T., and Delong, E. F.: The Microbial Engines That Drive Earth’s Biogeochemical  
732 Cycles, *Science*, 320, 1034–1039, <https://doi.org/10.1126/science.1153213>, 2008.
- 733 Gorsky, G., Ohman, M. D., Picheral, M., Gasparini, S., Stemmann, L., Romagnan, J.-B., Cawood, A., Pesant, S.,  
734 Garcia-Comas, C., and Prejger, F.: Digital zooplankton image analysis using the ZooScan integrated system,  
735 *Journal of Plankton Research*, 32, 285–303, <https://doi.org/10.1093/plankt/fbp124>, 2010.
- 736 Gorsky, G., Bourdin, G., Lombard, F., Pedrotti, M. L., Audrain, S., Bin, N., Boss, E., Bowler, C., Cassar, N.,  
737 Caudan, L., Chabot, G., Cohen, N. R., Cron, D., De Vargas, C., Dolan, J. R., Douville, E., Elineau, A., Flores, J.  
738 M., Ghiglione, J. F., Haëntjens, N., Hertaut, M., John, S. G., Kelly, R. L., Koren, I., Lin, Y., Marie, D., Moulin,  
739 C., Moucherie, Y., Pesant, S., Picheral, M., Poulain, J., Pujo-Pay, M., Reverdin, G., Romac, S., Sullivan, M. B.,  
740 Trainic, M., Tressol, M., Troublé, R., Vardi, A., Voolstra, C. R., Wincker, P., Agostini, S., Banaigs, B., Boissin,  
741 E., Forcioli, D., Furla, P., Galand, P. E., Gilson, E., Reynaud, S., Sunagawa, S., Thomas, O. P., Thurber, R. L. V.,  
742 Zoccola, D., Planes, S., Allemand, D., and Karsenti, E.: Expanding Tara Oceans Protocols for Underway,  
743 Ecosystemic Sampling of the Ocean-Atmosphere Interface During Tara Pacific Expedition (2016–2018), *Front.*  
744 *Mar. Sci.*, 6, 750, <https://doi.org/10.3389/fmars.2019.00750>, 2019.
- 745 Gove, J. M., McManus, M. A., Neuheimer, A. B., Polovina, J. J., Drazen, J. C., Smith, C. R., Merrifield, M. A.,  
746 Friedlander, A. M., Ehses, J. S., Young, C. W., Dillon, A. K., and Williams, G. J.: Near-island biological hotspots  
747 in barren ocean basins, *Nat Commun*, 7, 10581, <https://doi.org/10.1038/ncomms10581>, 2016.
- 748 Harris, R., Wiebe, P., Lenz, S., Skjoldal, H. R., Huntley, M.: ICES Zooplankton Methodology Manual, Elsevier,  
749 <https://doi.org/10.1016/B978-0-12-327645-2.X5000-2>, 2000.
- 750 Herdman, W.A., Variations in successive vertical plankton hauls at Port Erin. *Proc. And Trans. L’pool biol. Soc.*,  
751 Vol. 35, pp, 161-74, 1921.
- 752 Hidalgo-Ruz, V., Gutow, L., Thompson, R. C., and Thiel, M.: Microplastics in the Marine Environment: A  
753 Review of the Methods Used for Identification and Quantification, *Environ. Sci. Technol.*, 46, 3060–3075,  
754 <https://doi.org/10.1021/es2031505>, 2012.
- 755 Ikeda, T.: Metabolic rates of epipelagic marine zooplankton as a function of body mass and temperature, *Mar.*  
756 *Biol.*, 85, 1–11, <https://doi.org/10.1007/BF00396409>, 1985.



- 757 Imai, K. and Lehmann, H.: The oxygen affinity of haemoglobin Tak, a variant with an elongated beta chain,  
758 *Biochim Biophys Acta*, 412, 288–294, [https://doi.org/10.1016/0005-2795\(75\)90043-4](https://doi.org/10.1016/0005-2795(75)90043-4), 1975.
- 759 Jalabert, L.: ZooScan Protocol v1, <https://doi.org/10.17504/protocols.io.yxmvmk8j9g3p/v1>, 27 October 2021.
- 760 Jonas, T. D.: The volume of water filtered by a Continuous Plankton Recorder sample: the effect of ship speed,  
761 *Journal of Plankton Research*, 26, 1499–1506, <https://doi.org/10.1093/plankt/fbh137>, 2004.
- 762 Karlsson, T. M., Kärman, A., Rotander, A., and Hassellöv, M.: Comparison between manta trawl and in situ  
763 pump filtration methods, and guidance for visual identification of microplastics in surface waters, *Environ Sci*  
764 *Pollut Res*, 27, 5559–5571, <https://doi.org/10.1007/s11356-019-07274-5>, 2020.
- 765 Keen, E.: A Practical Designer's Guide to Mesozooplankton Nets, Available:  
766 <http://acsweb.ucsd.edu/~ekeen/resources/Choosing-a-Net.pdf>, 2013, last access: 12 November 2024.
- 767 Lombard, F., Boss, E., Waite, A. M., Vogt, M., Uitz, J., Stemmann, L., Sosik, H. M., Schulz, J., Romagnan, J.-  
768 B., Picheral, M., Pearlman, J., Ohman, M. D., Niehoff, B., Möller, K. O., Miloslavich, P., Lara-Lpez, A., Kudela,  
769 R., Lopes, R. M., Kiko, R., Karp-Boss, L., Jaffe, J. S., Iversen, M. H., Irsson, J.-O., Fennel, K., Hauss, H., Guidi,  
770 L., Gorsky, G., Giering, S. L. C., Gaube, P., Gallagher, S., Dubelaar, G., Cowen, R. K., Carloti, F., Briseño-Avena,  
771 C., Berline, L., Benoit-Bird, K., Bax, N., Batten, S., Ayata, S. D., Artigas, L. F., and Appeltans, W.: Globally  
772 Consistent Quantitative Observations of Planktonic Ecosystems, *Front. Mar. Sci.*, 6, 196,  
773 <https://doi.org/10.3389/fmars.2019.00196>, 2019.
- 774 Gehringer, J.W.: An all metal plankton sampler (model Gulf III), U.S. Fish and Wildl. Serv., spec. sci. Rep. Fish.,  
775 (88) 7-12, 1958.
- 776 Lombard, F., Bourdin, G., Pesant, S., Agostini, S., Baudena, A., Boissin, E., Cassar, N., Clampitt, M., Conan, P.,  
777 Da Silva, O., Dimier, C., Douville, E., Elineau, A., Fin, J., Flores, J. M., Ghiglione, J.-F., Hume, B. C. C., Jalabert,  
778 L., John, S. G., Kelly, R. L., Koren, I., Lin, Y., Marie, D., McMinds, R., Mériquet, Z., Metzl, N., Paz-García, D.  
779 A., Pedrotti, M. L., Poulain, J., Pujo-Pay, M., Ras, J., Reverdin, G., Romac, S., Rouan, A., Röttinger, E., Vardi,  
780 A., Woolstra, C. R., Moulin, C., Iwankow, G., Banaigs, B., Bowler, C., De Vargas, C., Forcioli, D., Furla, P.,  
781 Galand, P. E., Gilson, E., Reynaud, S., Sunagawa, S., Sullivan, M. B., Thomas, O. P., Troublé, R., Thurber, R.  
782 V., Wincker, P., Zoccola, D., Allemand, D., Planes, S., Boss, E., and Gorsky, G.: Open science resources from  
783 the Tara Pacific expedition across coral reef and surface ocean ecosystems, *Sci Data*, 10, 324,  
784 <https://doi.org/10.1038/s41597-022-01757-w>, 2023.
- 785 Longhurst, A. R.: TOWARD AN ECOLOGICAL GEOGRAPHY OF THE SEA, in: *Ecological Geography of the*  
786 *Sea*, Elsevier, 1–17, <https://doi.org/10.1016/B978-012455521-1/50002-4>, 2007.
- 787 Longhurst, A. R., Reith, A. D., Bower, R. E., and Seibert, D. L. R.: A new system for the collection of multiple  
788 serial plankton samples, *Deep Sea Research and Oceanographic Abstracts*, 13, 213–222,  
789 [https://doi.org/10.1016/0011-7471\(66\)91101-6](https://doi.org/10.1016/0011-7471(66)91101-6), 1966.
- 790 Picheral, M., Colin, S. and Irsson, J. O.: EcoTaxa, a tool for the taxonomic classification of images:  
791 <http://ecotaxa.obs-vlfr.fr>.
- 792 Mériquet, Z., Bourdin, G., Jalabert, L., Caray--Counil, L., Maury, J., Elineau, A., Pedrotti, M.-L., Gorsky, G., and  
793 Lombard, F.: Global scale surface meso-plankton and microplastics dataset collected with Manta Net and imaged  
794 with ZooScan during the Tara Pacific Expedition, <https://doi.org/10.17882/102537>, 2024a.
- 795 Mériquet, Z., Bourdin, G., Jalabert, L., Bun, O., Caray--Counil, L., Elineau, A., Gorsky, G., and Lombard, F.:  
796 Global scale surface meso-plankton dataset collected with High-Speed Net and imaged with ZooScan during the  
797 Tara Pacific Expedition, <https://doi.org/10.17882/102336>, 2024b.
- 798 Mériquet, Z., Kristan, N., Bourdin, G., Gorsky, G., Karp-Boss, L., and Lombard, F.: Global scale surface micro-  
799 plankton dataset collected with Bongo nets and imaged with FlowCam during the Tara Pacific Expedition,  
800 <https://doi.org/10.17882/102694>, 2024c.
- 801 Mériquet, Z., Bourdin, G., Jalabert, L., Bun, O., Caray--Counil, L., Elineau, A., Gorsky, G., and Lombard, F.:  
802 Global scale surface micro-plankton dataset collected with Deck Net and imaged with FlowCam during the Tara  
803 Pacific Expedition, <https://doi.org/10.17882/102697>, 2024d.
- 804 Mériquet, Z., Oddone, A., Le Guen, D., Pollina, T., Bazile, R., Moulin, C., Troublé, R., Prakash, M., De Vargas,  
805 C., and Lombard, F.: Basin-Scale Underway Quantitative Survey of Surface Microplankton Using Affordable  
806 Collection and Imaging Tools Deployed From Tara, *Front. Mar. Sci.*, 9, 916025,  
807 <https://doi.org/10.3389/fmars.2022.916025>, 2022.



- 808 Messié, M., Petrenko, A., Doglioli, A. M., Martinez, E., and Alvain, S.: Basin-scale biogeochemical and  
809 ecological impacts of islands in the tropical Pacific Ocean, *Nat. Geosci.*, 15, 469–474,  
810 <https://doi.org/10.1038/s41561-022-00957-8>, 2022.
- 811 Motoda, S.: Devices of simple plankton apparatus, 1959.
- 812 Pasquier, G., Doyen, P., Kazour, M., Dehaut, A., Diop, M., Duflos, G., and Amara, R.: Manta Net: The Golden  
813 Method for Sampling Surface Water Microplastics in Aquatic Environments, *Front. Environ. Sci.*, 10, 811112,  
814 <https://doi.org/10.3389/fenvs.2022.811112>, 2022.
- 815 Pedrotti, M. L., Lombard, F., Baudena, A., Galgani, F., Elineau, A., Petit, S., Henry, M., Troublé, R., Reverdin,  
816 G., Ser-Giacomi, E., Kedzierski, M., Boss, E., and Gorsky, G.: An integrative assessment of the plastic debris  
817 load in the Mediterranean Sea, *Science of The Total Environment*, 838, 155958,  
818 <https://doi.org/10.1016/j.scitotenv.2022.155958>, 2022.
- 819 Picheral, P., Colin, S. and Irissou, J. O.: EcoTaxa, a tool for the taxonomic classification of images:  
820 <http://ecotaxa.obs-vlfr.fr>, last access: 12 November 2024.
- 821 Piquv site: <https://sites.google.com/view/piqv/piqvmanuals/instruments-manuals>, last access: 1 November 2024.
- 822 Planes, S., Allemand, D., Agostini, S., Banaigs, B., Boissin, E., Boss, E., Bourdin, G., Bowler, C., Douville, E.,  
823 Flores, J. M., Forcioli, D., Furla, P., Galand, P. E., Ghiglione, J.-F., Gilson, E., Lombard, F., Moulin, C., Pesant,  
824 S., Poulain, J., Reynaud, S., Romac, S., Sullivan, M. B., Sunagawa, S., Thomas, O. P., Troublé, R., De Vargas,  
825 C., Vega Thurber, R., Voolstra, C. R., Wincker, P., Zoccola, D., and the Tara Pacific Consortium: The Tara Pacific  
826 expedition—A pan-ecosystemic approach of the “-omics” complexity of coral reef holobionts across the Pacific  
827 Ocean, *PLoS Biol.*, 17, e3000483, <https://doi.org/10.1371/journal.pbio.3000483>, 2019.
- 828 Platt, T., Denman, K.: The structure of pelagic ecosystems. *Rapp P-V Reun. Cons. Int. Explor Mer* 173:60-5,  
829 1978.
- 830 Sameoto, D., Wiebe, P., Runge, J., Postel, L., Dunn, J., Miller, C., and Coombs, S.: Collecting zooplankton, in:  
831 ICES Zooplankton Methodology Manual, Elsevier, 55–81, <https://doi.org/10.1016/B978-012327645-2/50004-9>,  
832 2000.
- 833 Sieracki, C., Sieracki, M., and Yentsch, C.: An imaging-in-flow system for automated analysis of marine  
834 microplankton, *Mar. Ecol. Prog. Ser.*, 168, 285–296, <https://doi.org/10.3354/meps168285>, 1998.
- 835 Skjoldal, H. R., Prokopchuk, I., Bagøien, E., Dalpadado, P., Nesterova, V., Rønning, J., and Knutsen, T.:  
836 Comparison of Juday and WP2 nets used in joint Norwegian–Russian monitoring of zooplankton in the Barents  
837 Sea, *Journal of Plankton Research*, 41, 759–769, <https://doi.org/10.1093/plankt/fbz054>, 2019.
- 838 Skjoldal, H. R., Wiebe, P., Postel, L., Knutsen, T., Kaartvedt, S., and Sameoto, D.: Intercomparison of  
839 zooplankton (net) sampling systems: Results from the ICES/GLOBEC sea-going workshop, *Progress in  
840 Oceanography*, 108, 1–42, <https://doi.org/10.1016/j.pocean.2012.10.006>, 2013.
- 841 Smith, P.E., Counts, R.C., Cutter, R.I.: Changes in filtering efficiency of plankton nets due to clogging under tow.,  
842 1968a.
- 843 Smith, P. E., Tranter, D. J., Filtration performance D.J. Tranter (Ed.), *Monographs on oceanographic methodology*  
844 2, Zooplankton sampling, UNESCO Press, Paris (1968), pp. 27-56, 1968b.
- 845 Steinberg, D. K. and Landry, M. R.: Zooplankton and the Ocean Carbon Cycle, *Annu. Rev. Mar. Sci.*, 9, 413–  
846 444, <https://doi.org/10.1146/annurev-marine-010814-015924>, 2017.
- 847 Tranter, D.J., Heron, A.C.: Experiments on filtration in plankton nets *Australian Journal of Marine and Freshwater  
848 Research*, 18, pp. 89-111, 1967.
- 849 Turner, J. T.: Zooplankton fecal pellets, marine snow, phytodetritus and the ocean’s biological pump, *Progress in  
850 Oceanography*, 130, 205–248, <https://doi.org/10.1016/j.pocean.2014.08.005>, 2015a.
- 851 Vandromme, P., Stemmann, L., Garcia-Comas, C., Berline, L., Sun, X., and Gorsky, G.: Assessing biases in  
852 computing size spectra of automatically classified zooplankton from imaging systems: A case study with the  
853 ZooScan integrated system, *Methods in Oceanography*, 1–2, 3–21, <https://doi.org/10.1016/j.mio.2012.06.001>,  
854 2012.
- 855 Von Ammon, U., Jeffs, A., Zaiko, A., Van Der Reis, A., Goodwin, D., Beckley, L. E., Malpot, E., and Pochon,  
856 X.: A Portable Cruising Speed Net: Expanding Global Collection of Sea Surface Plankton Data, *Front. Mar. Sci.*,  
857 7, 615458, <https://doi.org/10.3389/fmars.2020.615458>, 2020.
- 858 Wiebe, P. H., and Holland, W. R., PLANKTON PATCHINESS: EFFECTS ON REPEATED NET TOWS, 1968.



859 Wilkinson, M. D., Dumontier, M., Aalbersberg, Ij. J., Appleton, G., Axton, M., Baak, A., Blomberg, N., Boiten,  
860 J.-W., Da Silva Santos, L. B., Bourne, P. E., Bouwman, J., Brookes, A. J., Clark, T., Crosas, M., Dillo, I., Dumon,  
861 O., Edmunds, S., Evelo, C. T., Finkers, R., Gonzalez-Beltran, A., Gray, A. J. G., Groth, P., Goble, C., Grethe, J.  
862 S., Heringa, J., 'T Hoen, P. A. C., Hooft, R., Kuhn, T., Kok, R., Kok, J., Lusher, S. J., Martone, M. E., Mons, A.,  
863 Packer, A. L., Persson, B., Rocca-Serra, P., Roos, M., Van Schaik, R., Sansone, S.-A., Schultes, E., Sengstag, T.,  
864 Slater, T., Strawn, G., Swertz, M. A., Thompson, M., Van Der Lei, J., Van Mulligen, E., Velterop, J.,  
865 Waagmeester, A., Wittenburg, P., Wolstencroft, K., Zhao, J., and Mons, B.: The FAIR Guiding Principles for  
866 scientific data management and stewardship, *Sci Data*, 3, 160018, <https://doi.org/10.1038/sdata.2016.18>, 2016.  
867

868